USGS
science for a changing world

Documentation for the Southeast Asia Seismic Hazard Maps

By Mark Petersen, Stephen Harmsen, Charles Mueller, Kathleen Haller, James Dewey, Nicolas Luco, Anthony Crone, David Lidke, and Kenneth Rukstales

Administrative Report September 30, 2007

U.S. Department of the Interior
U.S. Geological Survey

U.S. Department of the Interior

DIRK KEMPTHORNE, Secretary

U.S. Geological Survey
Mark D. Myers, Director

U.S. Geological Survey, Reston, Virginia 2007
Revised and reprinted: 200x

For product and ordering information:
World Wide Web: http://www.usgs.gov/pubprod
Telephone: 1-888-ASK-USGS

For more information on the USGS—the Federal source for science about the Earth, its natural and living resources, natural hazards, and the environment:
World Wide Web: http://www.usgs.gov
Telephone: 1-888-ASK-USGS

Suggested citation:
Author1, F.N., Author2, Firstname, 2001, Title of the publication: Place of publication (unless it is a corporate entity), Publisher, number or volume, page numbers; information
on how to obtain if it's not from the group above.

Contents

Figures

Tables

Plate

Documentation for the Southeast Asia Seismic Hazard Maps

By Mark Petersen, Stephen Harmsen, Charles Mueller, Kathleen Haller, James Dewey, Nicolas Luco, Anthony Crone, David Lidke, and Kenneth Rukstales

Overview of Project

The U.S. Geological Survey (USGS) Southeast Asia Seismic Hazard Project originated in response to the 26 December 2004 Sumatra earthquake (M9.2) and the resulting tsunami that caused significant casualties and economic losses in Indonesia, Thailand, Malaysia, India, Sri Lanka, and the Maldives. During the course of this project, several great earthquakes ruptured subduction zones along the southern coast of Indonesia (fig. 1) causing additional structural damage and casualties in nearby communities. Future structural damage and societal losses from large earthquakes can be mitigated by providing an advance warning of tsunamis and introducing seismic hazard provisions in building codes that allow buildings and structures to withstand strong ground shaking associated with anticipated earthquakes. The Southeast Asia Seismic Hazard Project was funded through a United States Agency for International Development (USAID)—Indian Ocean Tsunami Warning System to develop seismic hazard maps that would assist engineers in designing buildings that will resist earthquake strong ground shaking. An important objective of this project was to discuss regional hazard issues with building code officials, scientists, and engineers in Thailand, Malaysia, and Indonesia. The code communities have been receptive to these discussions and are considering updating the Thailand and Indonesia building codes to incorporate new information (for example, see notes from Professor Panitan Lukkunaprasit, Chulalongkorn University in Appendix A).

Additional goals of the Project include:

- Developing seismic hazard maps that consider consensus input parameters for earthquake sources and ground shaking parameters obtained through workshop discussions.
- Building capacity of each country by training local scientists and engineers to update hazard maps.
- Producing outreach information for the public and policy makers on the seismic hazard issues and mitigation of associated risks.

The USGS achieved these objectives by developing hazard models and products and participating in four trips to Thailand and Indonesia, two trips to Malaysia, and one trip to India to hold workshops and training sessions. In addition, several coordination meetings were held with local USAID and U.S. embassy representatives: 4 April 2006 and 16 January 2007 with Orestes Anastasia; 21 January 2007 with Stacey Tighe (Jakarta,

Indonesia); and 18 July 2007 with Nina Minka (New Delhi, India) and Satish V. Kulkarni (New Delhi, India). These meetings helped set and modify priorities for the project and facilitate training meetings and workshops with local participants.

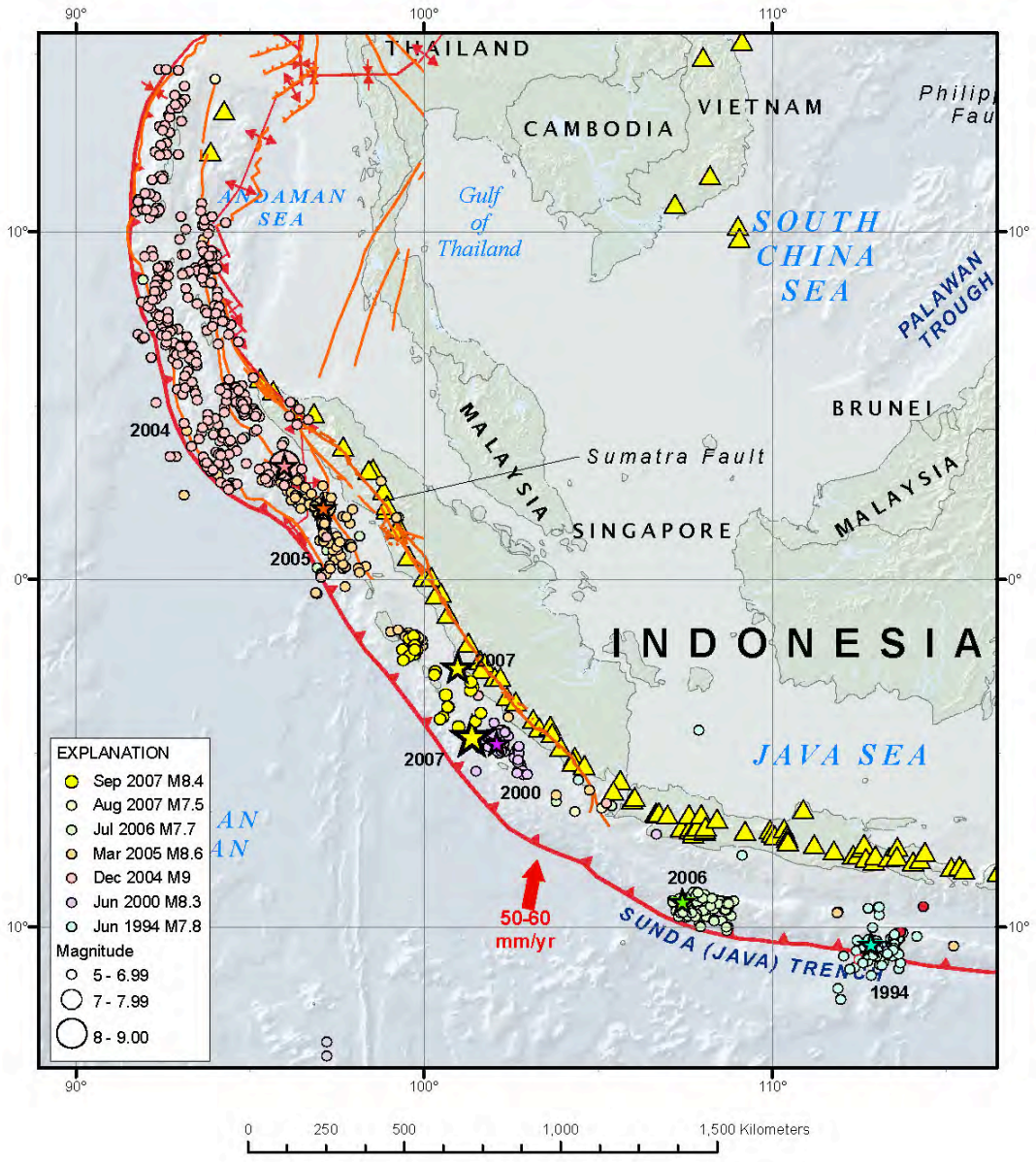

Figure 1. Map of subduction earthquakes (stars and circles) since 1994, volcanic centers (triangles), and generalized locations of major crustal faults (orange) and plate boundaries (red) in study region. Map courtesy of USGS National Earthquake Information Center (NEIC) Golden, CO

Hazard models and maps were produced at the USGS in Golden, Colo., using the methodologies established for producing the United States national seismic hazard maps (Frankel and others, 2002; Petersen and others, U.S. National Seismic Hazard Map Documentation at: http://earthquake.usgs.gov/research/hazmaps/). A new subduction

zone model was developed that considers historic seismicity, paleoseismic investigations, geodetic data, and ground motion studies. Seismicity catalogs and hazard models were updated to 2007. Fault maps were compiled for Thailand and for Indonesia through a contract with Kerry Sieh (California Institute of Technology and Danny Natawidjaja (Indonesian Institute of Science—the Sieh and Natawidjaja report on Indonesia is included in Appendix B). Fault maps were compiled and fault parameters were discussed at workshops held in Thailand and Indonesia. In addition, geology and shear-wave velocity maps and a seismic risk analysis were produced for a region surrounding Padang, Indonesia.

Project Activities in Thailand

During a series of workshops held in Bangkok, Thailand, the USGS and Thailand institutions involved in seismic hazard analysis worked together to develop consensus input parameters for a Thailand national seismic hazard map. Initial workshops were held by USGS (Mark Petersen) in June 2006 at Chulalongkorn University and the Asian Institute of Technology to coordinate Project activities. About 60 engineers, geologists, government officials, industry representatives, and academics participated. Some of the important topics addressed included: determining appropriate attenuation relations for the region near Bangkok, estimating maximum magnitudes of earthquakes on faults, and assessing data on fault recurrence.

During 16-19 January 2007, Kathleen Haller (USGS), Nicolas Luco (USGS), Charles Mueller (USGS), Mark Petersen (USGS), Ivan Wong (consulting seismic engineer from URS with experience in Thailand hazards), and several Thai engineers and earth-scientists, including Panitan Lukkunaprasit (Chulalongkorn University), Suwith Kosuwan (Department of Mineral Resources, and Disaster Warning Center), and Burin Wechbunthung (Thai Meteorological Dept.), provided training for about 150 local scientists and engineers (program is available at *http://earthquake.usgs.gov/research/hazmaps/whats_new/workshops/thailand/index.php*). The letter contained in Appendix A reports that almost all of the Thai seismic-hazard experts were present at these meetings. The USGS hazard computer codes and workshop notes were presented to all of the participants, and example hazard maps were run on about 30 PC workstations at Chulalongkorn University. This training was followed by a roundtable discussion between approximately 35 participants that focused on specific hazard map inputs and methodologies.

Three additional days of training were provided by USGS (Mark Petersen) from 26–28 June 2007 on new updated seismic hazard codes. A final workshop on 29 June 2007 included about 35 invited participants and focused on the final input parameters and hazard maps. Participants expressed their desire for future work with the USGS on the establishing a basis for the maximum magnitudes of earthquakes on major faults in Thailand and a more detailed analysis of fault parameters for the Three Pagodas fault, which is the primary contributor to hazard in Bangkok. In addition, discussions were held regarding the most appropriate attenuation relations for Bangkok. The USGS evaluated the input data, developed documentation, and updated the draft maps during August and September 2007.

Project Activities in Indonesia

USGS seismic hazard maps for Indonesia (Petersen and others, 2004) suggest significantly higher ground motions than the current Indonesia building code. An introductory workshop was held during June 2006 in Bandung, Indonesia, that included about 15 engineers and earth-scientists who had previously produced hazard maps for Indonesia and members of the Public Works Department who have responsibility for producing the current building codes. The focus of this workshop was to determine why the Petersen and others (2004) maps were higher than the current building code maps. Five different Indonesia hazard maps were compared and contrasted during the workshop by: Masyhur Irsyam (Institut Teknologi Bandung); Teddy Boen (structural engineering consultant and board member of the Worldwide Seismic Safety Initiative); Engkon Kertapati (Geological Survey Indonesia); Maryoko Hadi (Public Works Dept); and Mark Petersen (USGS). Participants agreed that the USGS would produce a regional hazard model and assist the Indonesian seismic hazard group at the Institut Teknologi Bandung (led by Masyhur Irsyam) in installing USGS hazard codes on their computers and developing a new hazard map for Indonesia that would be considered in revising the seismic design criteria for the Indonesian building code.

The USGS (Stephen Harmsen and Mark Petersen) provided training on USGS hazard codes for about 30 scientists and engineers between 10 and 14 July 2007 in Bandung, Indonesia. Seismic hazard issues and methodologies were also presented by USGS (Mark Petersen) between 12and 13 July 2007 to about 30 faculty, students, and professionals at the Gadjah Mada University in Jogyakarta (hosted by Dwikorita Karnawati, Professor of Geology). In addition, a seismic hazard workshop was held in Bandung that involved about 35 government officials responsible for building codes as well as the Indonesia Geological Survey, the BMG (responsible for earthquake monitoring), and several academic institutions. The workshop discussions focused on the reasons why Indonesia needs a new building code. Participants generally agreed that new hazard values should be considered in future updates of the building codes.

Another workshop and training session was held on 24 August 2007 as part of the Indonesian Society of Civil and Structural Engineers (HAKI) annual meeting. USGS (Nicolas Luco) presented a keynote talk at the annual meeting of the Indonesian Society of Civil and Structural engineers to about 500 engineers on the new USGS hazard and risk maps. In addition, a final USGS workshop involving about 25 participants was held in Jakarta following the HAKI annual meeting. Danny Natawidjaja (Indonesian Institute of Science), Masyhur Irsyam, and Dradjat Hoedajanto provided an Indonesia perspective on seismic hazard and USGS hazard experts (Nicolas Luco and Oliver Boyd) led discussions and training of the new hazard and risk maps developed by the USGS. These discussions focused on the current lack of paleoseismic data for active faults in Indonesia, particularly on the island of Java, and the types of infrastructure for which the standard return periods in probabilistic seismic hazard estimates could be applied. The Indonesian colleagues have expressed interest in further collaboration with the USGS on seismic hazard issues.

Project Activities in Other Countries

Two USGS workshops were also held in Malaysia during June 2006 and July 2007 that included building code officials and representatives from several universities.

In addition, discussions were held at the Tsunami Warning Center of the Malaysia Meteorological Department. These workshops were organized and led by USGS (Mark Petersen) and were not part of the work funded by USAID. Like others that participated in the workshops, earthquake hazard and building code experts in Malaysia expressed similar interest in future updates of their building codes. Dr. Azlan Adnan of the Universiti Teknologi Malaysia will lead this effort. These groups have requested that the USGS review the future Malaysia seismic hazard maps that will be implemented in the building code.

Mark Petersen and Kishor Jaiswal (structural engineering contractor, USGS) convened meetings in Delhi, India, to discuss future collaboration between the USGS and the Indian National Disaster Management Agency (NDMA), the Meteorological Agency (Atindra K. Shukla), and the Indian Institute of Technology, Bombay (Ravi Sinha, professor). These groups expressed interest in learning about the new hazard technologies being developed and implemented in the United States. The Meteorological Agency is responsible for earthquake monitoring and developing urban and regional hazard maps for India. Meetings held with members of the NDMA (B. Bhattacharjee, Vinod C. Menon, K. M. Singh, and others) involved discussions with public policy makers regarding the need to establish formal standards for urban hazard and engineering products that would affect urban planning. The group would like to establish further links to the USGS hazard mapping group through a Memorandum of Understanding (MOU).

Seismic hazard maps and input parameters are described in the main text of this report and available on the national seismic hazard mapping project website: *http://earthquake.usgs.gov/research/hazmaps/*. This documentation serves to provide guidance to engineers and scientists in Thailand, Malaysia, and Indonesia for updating their maps. In addition, a USAID fact sheet, Fact sheet: Scientists Develop Seismic Hazard Maps to Guide Safe Building Practices in Earthquake Zones, US IOTWS Program August, 2006, was developed to provide further hazard information (http://www.iotws.org/ev_en.php?ID=1274_201&ID2=DO_TOPIC).

Introduction

The USGS Southeast Asia Seismic Hazard Project was funded under the USAID—Indian Ocean Tsunami Warning System Program to develop new hazard maps as a resource for structural engineers in designing seismically resistant buildings following the devastating tsunami of 2004. In this hazard assessment, we update the Petersen and others (2004) hazard model for Southeast Asia by revising earthquake catalogs, developing new seismotectonic models, implementing new fault models, and incorporating new ground-motion prediction equations. In addition, we calculated the hazard using the updated methodologies that have been applied in the latest United States National Seismic Hazard Maps for peak ground acceleration (PGA) and spectral accelerations with hazard levels of 2-percent and 10-percent probabilities of exceedance in 50 yr (Frankel and others, 2002; Petersen and others, 2007; U.S. National Seismic Hazard Map Documentation at: *http://earthquake.usgs.gov/research/hazmaps/*). As far as we know, these are the first spectral acceleration hazard maps published for this region; these maps are essential for implementing the latest International Building Code design criteria.

The maps presented here differ significantly from many pre-existing maps of peak horizontal ground accelerations, so it is important that these differences be discussed in an open forum with local experts. Changes in the seismic hazard maps were discussed at a series of workshops held during 2006 and 2007: Bangkok, Thailand (March 2006, January 2007, and June 2007); Kuala Lumpur, Malaysia (April 2006 and July 2007); and Bandung, Indonesia (April 2006, July 2007, and August 2007). These maps and the underlying parameters and methodologies are being considered as input into several national building codes.

Previous regional hazard models for Southeast Asia were produced by Shah and Boen, unpublished, 1996), by the Global Seismic Hazard Assessment Program (Giardini, 1999), Megawati and Pan (2001), Adnan and others (2002), and Petersen and others (2004). For Thailand, the building codes incorporate seismic hazard information for the northern portion but not the southern portion of the country near Bangkok (personal communication Panitan Lukkunaprasit, 2007). Indonesia has implemented building code maps for peak ground acceleration at 10-percent probability of exceedance in 50 yr based on four different hazard models (personal communication, Teddy Boen, 2006).

The Global Seismic Hazard Assessment Program (GSHAP) assessment for southeast Asia is for peak ground acceleration with a 10-percent probability of exceedance in 50 yr hazard level (McCue, 1999). These maps are based mostly on the unpublished work of Shah and Boen that incorporates the Preliminary Determination of Epicenters (PDE) catalog to determine earthquake rates on the subduction zone and slip rates to determine the frequency of earthquakes along the Sumatra fault. Two ground-motion prediction equations were used to estimate the ground-shaking hazard in a probabilistic framework. Additionally, several deterministic scenario hazard models have been produced across the region including models that assess the ground motion due to a great Sumatran subduction earthquake scenario in Singapore (Megawati and Pan, 2001) and in Malaysia (Adnan and Yusof, 2001).

In this report we discuss the seismotectonics of southeast Asia, describe a new seismic hazard model, develop the rationale for a local risk analysis for Padang, Indonesia, and present various maps and graphs that are helpful in understanding the seismic hazard across this region.

Seismotectonics

Southeast Asia is a region of variable seismic hazard, ranging from high seismic hazard associated with the subduction process beneath the Indonesian and Philippine archipelagos to moderately low seismic hazard across a large stable region that contains the Malaysian peninsula. The Indonesian island chain is characterized by widespread volcanic activity and earthquake activity (figs. 1 , 2, and 3) resulting from the sliding of the India and Australia tectonic plates beneath the Sunda and Burma tectonic plates. Reverse, thrust-, strike-slip, and normal-focal mechanisms are reported within the region (fig. 4). The Sunda subduction zone (fig. 1) produces thrust-fault earthquakes on the interfaces between plates, earthquakes within the subducted India and Australia plates that extend down to depths of hundreds of kilometers, intraplate normal-fault and reverse-fault earthquakes within the shallow India and Australia plates, and shallow seismicity within the upper 30 km of the overriding Sunda and Burma plates. Additional

crustal faults occur within the Sunda plate well to the north and east of the Sunda subduction zone.

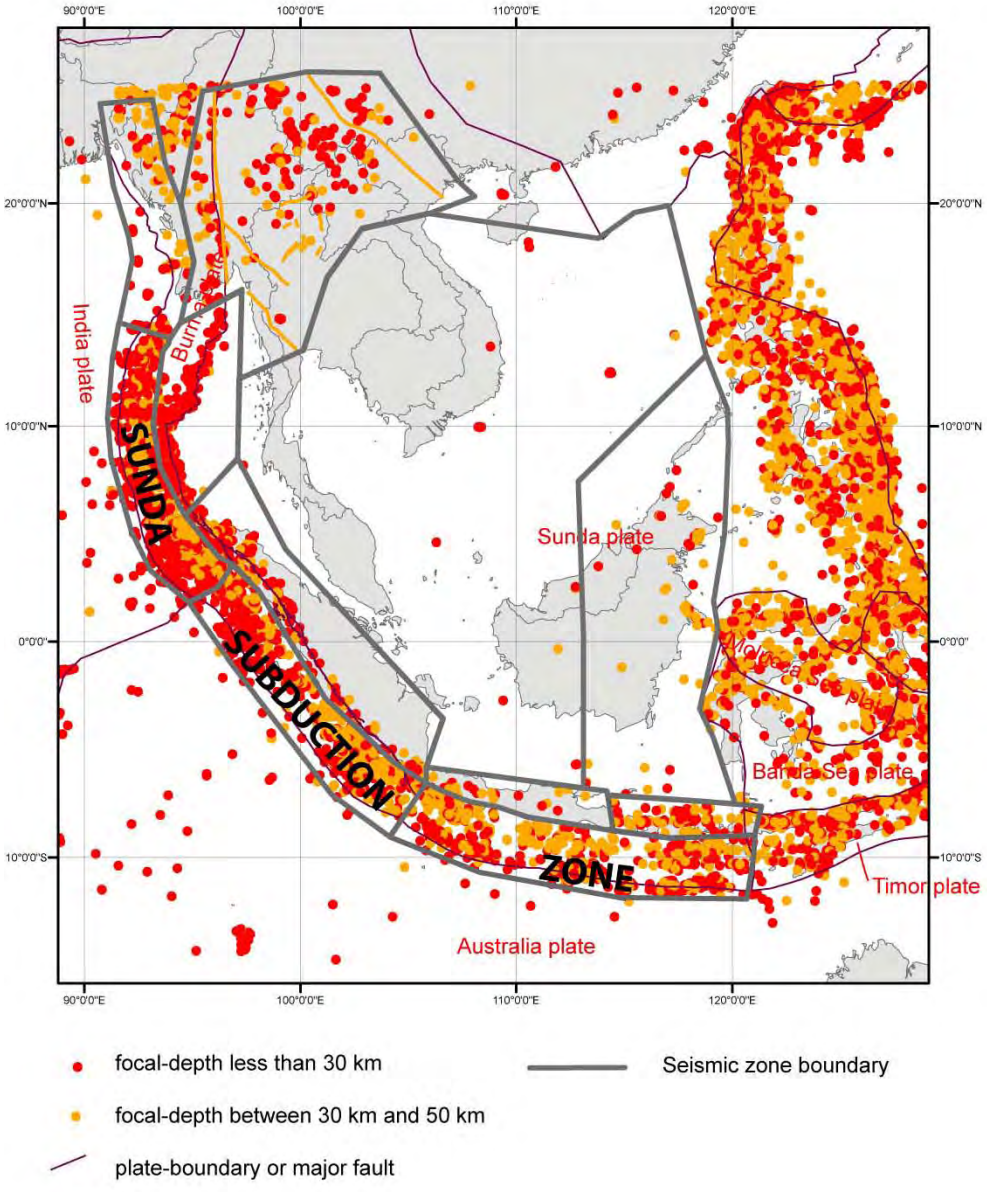

Figure 2. Map of shallow-depth earthquakes in the region of this study, with epicenters of shallow-focus earthquakes (focal depth less than 50 km) for the period 1964–2005 determined by the methodology of Engdahl and others (1998). Plate boundaries are generalized from Bird (2003), with some modification in the western part of the map. The southern boundary of the Burma plate is taken to be the southern end of the rupture zone of the 2004 Sumatra-Andaman Islands earthquake. The boundary between the Burma plate and India plate offshore of the Andaman Islands and Burma is from Pubellier and

others (2003) as are the positions of faults beneath the Andaman Sea. Seismic zones are labeled in Figure 5.

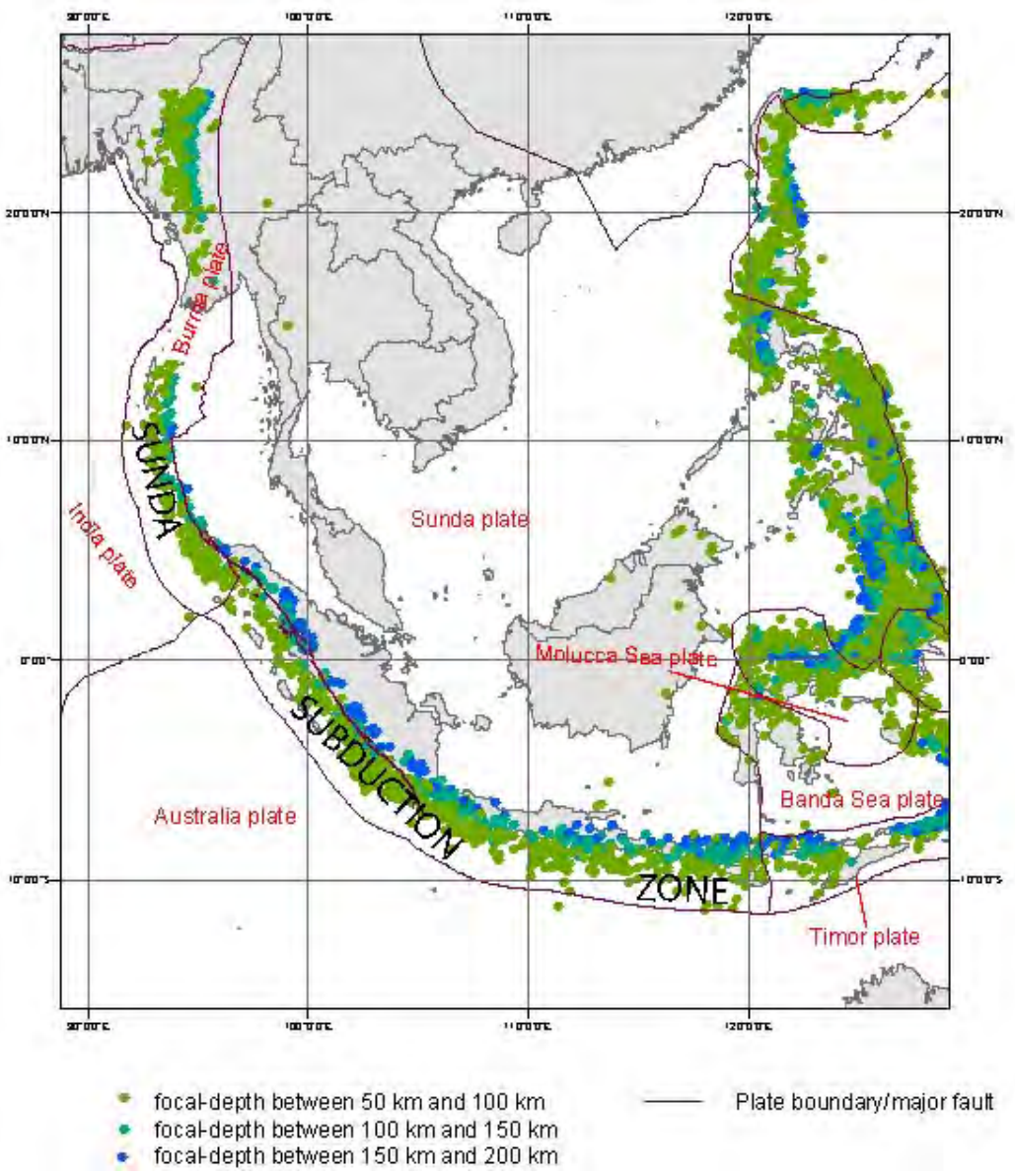

Figure 3. Map of epicenters of earthquakes having focal depths between 50 km and 200 km for the period 1964–2005, determined by the methodology of Engdahl and others (1998). Plate boundaries are as in Figure 1.

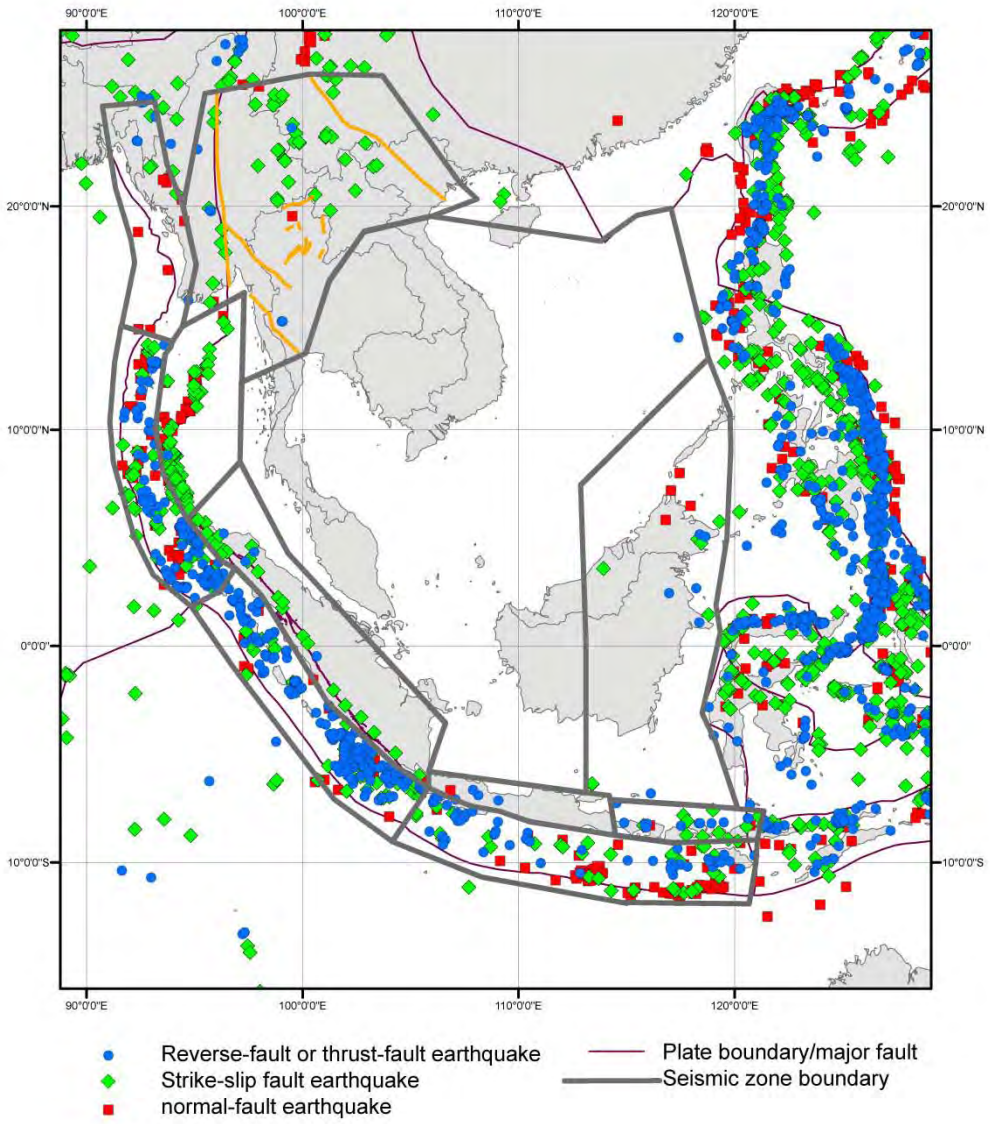

Figure 4. Map of shallow-depth earthquakes in study area, with epicenters of shallow-focus earthquakes (<50 km) for which Harvard Centroid Moment Tensor solutions are available, as determined by the methodology of Dziewonski and others (1980). Seismic zones are labeled in Figure 5.

Sunda Subduction Zone

For purposes of seismic hazard mapping, we divide the Sunda subduction zone into four major sections: the Burma, Northern Sumatra-Andaman, Southern Sumatra, and Java zones (fig. 5). The Burma zone corresponds to the subduction of the India plate beneath the Burma plate and the Burma orogen in western Burma. Le Dain and others (1984) and Guzman-Speziale and Ni (1996) note the absence of instrumentally recorded earthquakes with locations and focal-mechanisms corresponding to slip on the interface between the India plate and the northern Burma plate or Burma orogen. The lack of

recent seismicity may be due to the zone being permanently incapable of producing great earthquakes or it may be due to the plate having been locked during the relatively short record of instrumental seismicity, but still accumulating elastic strain that might be released in a future great earthquake. Socquet and others (2006) present Global Positioning Systems (GPS) observations that suggest the plates are locked and accumulating strain due to oblique northeastward convergence of about 20 mm/yr along the Arakan Trench on the west coast of Burma. Although this model is not a unique interpretation of the GPS data, it is favored by Socquet and others (2006) and would imply that this region has a high long-term potential for the occurrence of great underthrust earthquakes.

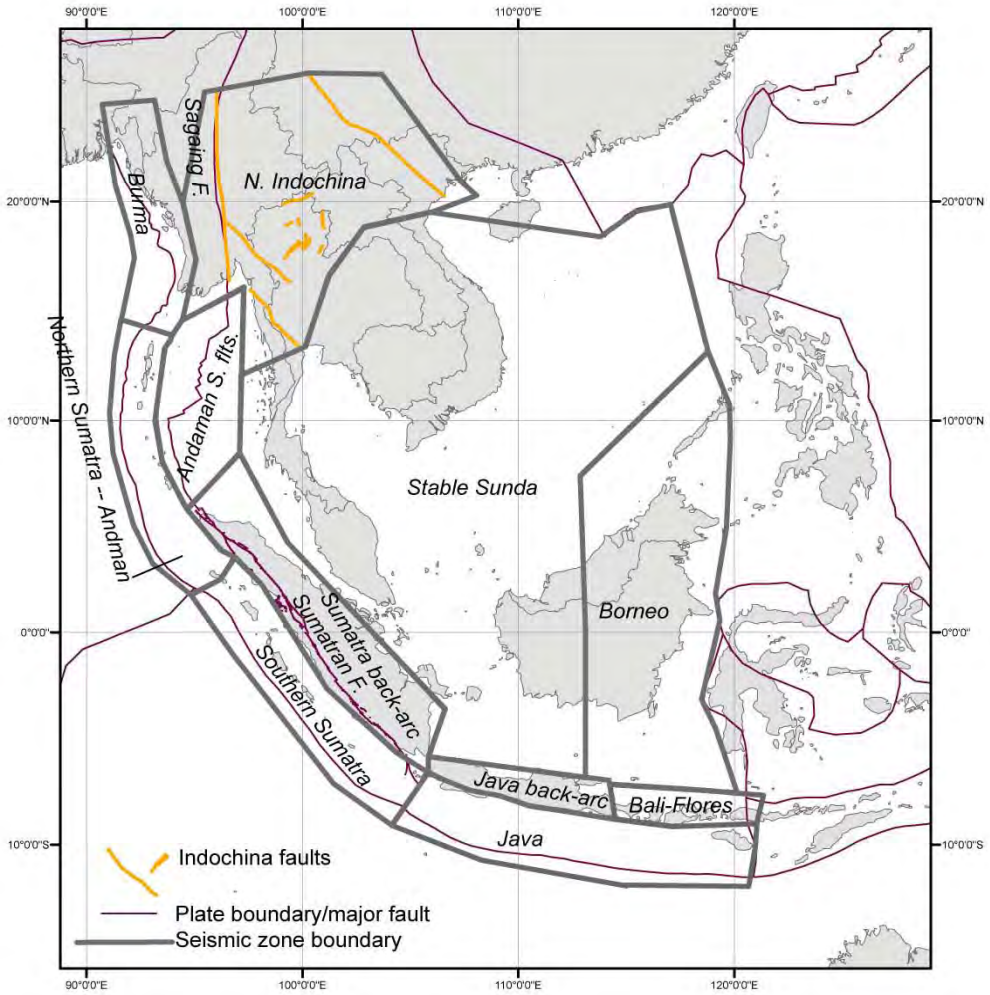

Figure 5. Map of shallow-depth earthquake source zones (labeled) that were considered for this study. Plates are not labeled in this figure, to avoid confusion with earthquake source zones; plates are labeled in Figures 2 and 3. The Sumatran fault is from Sieh and Natawidjaja (2000).

The Northern Sumatra-Andaman zone encompasses offshore northern Sumatra, the Nicobar Island chain, and the Andaman Island chain. In this area, the Indian plate is subducting obliquely beneath the Burma plate. This zone trends nearly north-south as opposed to the nearly east-west trending section of the Sunda subduction zone near the

island of Java, which we are calling the Java zone. Here the estimated rate of subduction is 20 mm/yr to 40 mm/yr, with the higher rates to the south (Rajendran and others, 2007; Socquet and others (2006); and Chlieh and others, 2006). The Northern Sumatra-Andaman zone last ruptured in the 26 December 2004 Sumatra earthquake (M9.2). The seismic/geodetic model of Chlieh and others (2006), however, shows that some patches of the subduction zone interface between lat. 2° N. and 14° N. apparently did not rupture during the December 2004 mainshock or during the month following the mainshock. Some of these patches are large enough to produce sizeable earthquakes, if they are capable of accumulating and releasing elastic strain.

The Southern Sumatra zone encompasses one of the most seismically active plate tectonic margins in the world, and accommodates oblique north-eastward convergence of about 50 mm/yr between the Australia plate and the Sunda plate (fig. 1). Large subduction zone (plate-interface) earthquakes occurred in 1833 (~M9.0±0.2), 1861 (M8.5), and 2000 (M_w7.9), 2005 (M_w8.6) (Natawidjaja and others, 2006; Newcomb and McCann, 1987; Zachariasen and others, 1999), and 2007 (Mw 8.4, 7.9).

Within the Java zone, earthquakes have produced damage from either shaking or tsunamis as the result of thrust-faulting on the plate interface and faulting within the Australia or Sunda plates. The largest interface thrust earthquakes in the Java-Timor zone since 1900 were the 1994 June 2 (M_w7.8) and 2006 July 17 (M_w7.7) earthquakes, both of which produced destructive tsunamis but neither of which caused recognized damage from shaking. These earthquakes were an uncommon type of earthquake, commonly called “tsunami earthquake” (*e.g.*, Polet and Kanamori, 2000; Ammon and others, 2006). “Tsunami earthquakes” produce relatively low-levels of the high-frequency energy that cause shaking damage to buildings but are unusually efficient at generating tsunami waves.

Although the seismological evidence is clear that the Java zone can produce interplate thrust-fault earthquakes with magnitudes approaching M_w8.0, there have been no cataloged earthquakes of M_w8.0 or larger in the Java zone that appear likely to have been due to thrust-faulting on the interface (Newcomb and McCann, 1987) since the mid nineteenth century. Lay and others (1982) and Newcomb and McCann (1987) suggest that this region of the eastern Sunda arc is much less likely to experience great underthrust earthquakes than the western Sunda arc. Smaller earthquakes are speculated because of weak coupling at the plate interface that may be due to the nature of the older high-density subducting lithosphere beneath the Java zone. Geodetic observations (Simons and others, 2007) are consistent with weak coupling on the subduction interface.

The largest earthquake in the Java zone since 1900 was the 19 August 1977 (M_w8.3) earthquake, which was an intraplate earthquake occurring within the subducting Australia plate rather than an interplate earthquake occurring on the thrust interface between the Australia plate and the overriding Sunda plate. The 1977 earthquake produced a destructive tsunami; little or no damage resulted from shaking due to its distance offshore.

Sunda Plate

The regions of the Sunda plate adjacent to the Sunda subduction zone (the regions designated ‘Sumatra back-arc,’ ‘Java back-arc,’ and ‘Bali-Flores’ in fig. 5) have a moderate to high rate of earthquake activity.

The "Bali-Flores" zone is a back-arc thrust zone (McCaffrey and Nabelek, 1987) lying within Bird's (2003) Sunda plate. McCaffrey and Nabelek (1987) suggest that compressional stresses responsible for the back-arc thrusting are a consequence of the impingement of the buoyant Roo Rise on the Java trench south of Java. The largest instrumentally recorded earthquake in this zone had M_w7.7.

Non Sumatran fault earthquakes within the 'Sumatra back-arc' zone and earthquakes in the 'Java back-arc' zone reflect strains that are generated at the plate boundary but that are not accommodated by thrust-faulting at the plate interface or (in Sumatra) by slip on the Sumatran fault. This earthquake activity occurs on faults that have either not been geologically mapped or that have not been studied to the extent that their current rates of activity can be estimated from geologic evidence. The importance of understanding these faults was emphasized by the Mw 6.3 Yogyakarta earthquake of May 26, 2006, which occurred on such a fault.

The margin of the Sunda plate lying in eastern Borneo ('Borneo' zone in fig. 5) has a moderate rate of earthquake activity, and geodetic evidence of tectonic deformation is reported by Rangin and others (1999) and Simons and others (2007). The largest earthquake in the zone was the earthquake of April 19, 1923, which had a magnitude of 6.9 (Engdahl and Villasenor, 2002).

The Malaysian peninsula, western Borneo, and portions of eastern Thailand are located within the stable core of the Sunda plate and are characterized by low seismicity and strain rates. Within the boundary of this broad 'Stable Sunda' zone, only about 20 well-located earthquakes with magnitude greater than M5 occurred during the years 1964 to 2007. Geodetic data also indicate that strains measured within the Stable Sunda zone are low (Rangin and others, 1999; Simons and others, 2007). This region, however, is situated about 300-600 km from the Sumatran faults that have historically produced earthquakes with ground motions that were felt in buildings in Singapore and Kuala Lumpur (Pan and Sun, 1996; Pan, 1997; Pan and others, 2001).

Earthquakes Within Deep Subducted Plates

Figure 3 shows the distribution of earthquakes having depths between 50 km and 200 km. Most of these earthquakes occurred within tectonic plates rather than at their plate boundaries, and most represent deformation within subducted plates. The study region also experiences earthquakes deeper than 200 km, down to focal depths of about 650 km. Because of their remoteness from the ground surface, earthquakes deeper than 200 km typically cause little damage, but large earthquakes deeper than 200 km may be felt at great distance from their hypocenters.

Southeast Asia Hazard Model

The seismic hazard maps for Southeast Asia described in this report incorporate a similar methodology previously used in Sumatra (Petersen and others, 2004), but for this version we updated the earthquake catalog, accounted for random earthquakes across several depth ranges, incorporated new consensus-based crustal fault parameters, developed new subduction zone models that take into account the 2004 (M9.2) earthquake, and applied new attenuation relations. Ground motions are modeled using attenuation relations appropriate for the style of faulting and characteristics of the crust.

We apply the same general methodologies that were used to calculate the United States National Seismic Hazard Maps (Frankel and others, 1996; Frankel and others, 2002).

Earthquake Catalog

Earthquake catalogs are used to estimate future seismic activity from the locations and rates of past earthquakes. Even small earthquakes that are not felt but only detected by seismographs can be used; from the locations and frequency-magnitude distributions of past earthquakes we can estimate the locations and rates of future larger shocks that dominate the hazard. In most parts of the world the seismic record is too short to include a complete sample of these larger, rarer shocks.

For this study we compiled a new catalog of instrumentally recorded earthquakes by combining four pre-existing global catalogs: (1) the IASPEI Centennial catalog compiled by Engdahl and Villaseñor (2002); (2) the catalog originally compiled by Engdahl, van der Hilst, and Buland (1998), and updated by Engdahl; (3) the USGS/NEIC Preliminary Determination of Epicenters on-line catalog (*http://neic.usgs.gov*); and (4) the International Seismological Centre on-line catalog (*http://www.isc.ac.uk*). In the following we refer to these source catalogs as EVC, EHB, PDE, and ISC, respectively. Each has unique strengths and weaknesses, and none is considered complete enough to use alone as a basis for the hazard analysis. They overlap considerably in coverage, and procedures that incorporate our judgment about source-catalog reliability are used to cull duplicate entries. The combined catalog covers an area from long. 88° E. to long. 122° E. and lat. 17° S. to lat. 26° N.

A single magnitude is selected for each earthquake from either the: (1) reported moment magnitude (M_w), (2) 20-second surface-wave magnitude (M_s), (3) the short-period P-wave magnitude (m_b), or (4) another magnitude, in that order of preference. Magnitudes are converted to moment magnitude (when possible) using relations published by Utsu (2002) and Sipkin (2003). We estimate the following completeness levels for the catalog: (1) for depth less than or equal to 50 km, M4.0 since about 1995, M4.5 since 1990, and M5.0 since 1964; (2) for depths greater than 50 km and less than or equal to 100 km, M4.5 since 1995, and M5.0 since 1964; and (3) for depths greater than 100 km and less than or equal to 250 km, M4.5 since 1990 and M5.0 since 1964.

A basic assumption of our seismic hazard methodology is that earthquake sources are independent. Thus, catalogs that are used to estimate future seismic activity must be declustered, or free of dependent events such as foreshocks and aftershocks. We apply the procedure of Gardner and Knopoff (1974) to eliminate foreshocks and aftershocks from the catalog. Gardner and Knopoff identified durations, T, and dimensions, L, as functions of mainshock magnitude, M, for a set of California data, and fit least-upper-bound envelopes to the data of the form: log T or log L = a M+ b. Following each earthquake in the chronologically ordered catalog, we scan for events within a [T(M),L(M)] window. If an event with magnitude less than or equal to M is found, it is deleted as an aftershock. For example, after a magnitude 6.0 earthquake, any smaller earthquake found within 510 days and a radius of 54 kilometers is deleted. If an event with magnitude greater than M is found, the original earthquake is deleted as a foreshock.

The combined catalog, after removal of duplicates, contains about 6710 records greater than or equal to M5 (1964–2006). Declustering eliminates about 59 percent of the events. Of the remaining approximately 2770 mainshocks, roughly 510 are contributed

by EVC, 1510 by EHB, 340 by PDE, and 410 by ISC. The declustered catalog is used to compute seismicity rates as described below.

Earthquake Source Model

The earthquake source model is composed of background seismicity, subduction zone segments, and crustal faults (see various input parameters in Tables 1, 3, and 4).

Table 1. Regional source model.

Source Zones	Minimum magnitude	Maximum magnitude	Recurrence (cumulative a-value and area of zone – or annual recurrence for characteristic earthquake)	b-value	Weight
1. Background seismicity					
Shallow (0-50 km)[1]	5.0	7.0	Smoothed seismicity	1.0	1.0
Intermediate (50-100, set at 60 km)	5.0	7.8	Smoothed seismicity	1.0	1.0
Intermediate (100-150, set at 100 k)	5.0	7.8	Smoothed seismicity	1.0	1.0
Deep (150-200 km, set at 150 km)	5.0	7.8	Smoothed seismicity	1.0	1.0
Deep (200-250 km, set at 200 km)	5.0	7.8	Smoothed seismicity	1.0	1.0
			Smoothed seismicity		
2a. Sunda smoothed seismicity	5.0	7.0	4.80/4,283,820 km^2	1.021	0.5
2b. Sunda constant seismicity	5.0	7.0		1.021	0.5
3. Crustal fault models					
Thailand	5.0	Mmax-Table 3	Table 3		1.0
Indonesia	5.0	Mmax- Table 2	Table 2		0.25 for 4 models
4. Sunda subduction zone					
Java-Sumatra-Andaman (GR)	7.1	9.1	6.29/1,427,270 km^2	1.014	0.333
Java-Sumatra-Andaman (GR)	5.0	7.0			0.333
Java (GR)	7.1	9.2	6.38/578,080 km^2	1.097	0.667
Java (GR)	5.0	7.0	6.38/578,080 km^2		0.667
Southern Sumatra (Char)		9.2	0.003/yr		0.667
Southern Sumatra (GR)	5.0	7.0	5.48/470,340 km^2	0.936	0.667
Northern Sumatra-Andaman (Char)		9.2	0.001/yr		0.667
Northern Sumatra-Andaman (GR)	5.0	7.0	5.15/378,860 km^2	0.959	0.667
Burma (GR)	7.1	9.2	5.72/325,070 km^2	1.190	0.667
Burma (GR)	5.0	7.0	5.72/325,070 km^2	1.190	0.667

[1] Shallow background seismicity (0-50 km) does not include region of the Sunda subduction zone or the Sunda plate zone. Char and GR represent characteristic and Gutenberg and Richter magnitude-frequency distributions.

Background Seismicity Model

Background seismicity in the model accounts for random earthquakes on unmapped faults and smaller earthquakes on mapped faults. We include two types of background seismicity: (1) gridded models that are based on spatially smoothed earthquake rates and (2) a background zone that accounts for a constant low rate of earthquakes across a broad Sunda plate. Background sources are based on the declustered (dependent events removed) earthquake catalog that begins in 1964. This model accounts for the observation that larger earthquakes ($M \geq 5$) occur near smaller ($M \geq 4$ or 5) earthquakes.

Gridded seismicity included in the model is based on earthquakes at five depth intervals (shallow 0-50 km, intermediate depth 50–100 km and 100–150 km, and deep 150–200 km and 200–250 km). A truncated-exponential or Gutenberg-Richter (Gutenberg and Richter, 1944) magnitude-frequency distribution between M5.0 and M7.0 is used to model rates for different sizes of earthquakes in each grid cell or zone. Parameters of the magnitude-rate distribution (regional b-values and a-values in cells or zones) are computed using a maximum-likelihood method (Weichert, 1980). For the smoothed seismicity models the earthquake rates in cells are spatially smoothed using a two-dimensional Gaussian smoothing operator with 50 km correlation distance. This procedure yields a magnitude-frequency distribution for each grid point separated by 0.1 degrees in longitude and latitude.

A major limitation of the smoothed seismicity model is that we only have a 36-yr catalog, which is very short with respect to earthquake recurrence rates on faults. The short record probably does not represent all possible future earthquakes in these regions. In order to compensate for the short historical record, we developed a second model, the background zone model, which assumes that the entire zone can have a random earthquake with a constant rate determined from the historical seismicity distributed over the broad zone. These two models were weighted 50-50 in the hazard analysis for the Malaysian peninsula.

The background zone includes the interior of the Sunda plate that has been very inactive seismically, with only five events occurring across this broad region. The earthquakes are too sparse to define any linear pattern to suggest the presence of a tectonically active structure dividing the Sunda plate into smaller units, and GPS data have not been able to detect significant deformation within the region (Rangin and others, 1999). The largest historical earthquake observed within the Stable Sunda zone was a M5.8 event. Consistent with USGS treatment of tectonically stable regions in the most recent United States National Seismic Hazard Maps, we take M7.0 as the size of the maximum plausible earthquake in this zone. This value corresponds to the magnitude of the largest earthquakes that have occurred in previously quiescent, generally tectonically stable, regions of plate interiors in other parts of the world. The calculated b-value is 1.08, but this value has very high uncertainty because of the low rate seismicity. We have applied a b-value of 1.0 for this zone based on the regional constraints.

The Sunda Subduction Zone Model

The megathrust Sunda subduction zone accounts for the largest earthquakes in the model, up to M9.2, the size of the 2004 Sumatra earthquake. The characteristics of earthquakes along the subduction zone vary along the strike of the fault. Great subduction

earthquakes in the model extend down 50 km, typical of cold descending slabs in this and other global subduction zones (Table 1). The rate of large earthquakes expressed in the model varies according to the historical earthquake rate and paleoseismic data on recurrence of great earthquakes.

We divide the Sunda subduction zone into four sections based on seismicity characteristics: Burma, Northern Sumatra-Andaman, Southern Sumatra, and Java (fig. 5). We consider several models for the subduction zones (Table 1): (1) models of constant seismicity M5.0-7.0 across each of the four different sections separately, (2) a model that accounts for constant seismicity M5.0-7.0 across the combined three sections: Java, Southern Sumatra, and Northern Sumatra-Andaman sections, (3) models that account for constant seismicity rate for M7.1-9.1 or 9.2 on each of the four different sections, (4) a model that accounts for constant seismicity rate M7.1-9.1 across the three combined sections: Java, Southern Sumatra, and Northern Sumatra-Andaman sections, (5) characteristic models that account for M9.2 earthquakes like the 2004 event on the Northern Sumatra-Andaman or on the Southern Sumatra sections.

The Burma section of the subduction zone, also known as the Arakan section, extends northward into Myanmar. GPS observations by Socquet and others (2006) were interpreted as (1) wrench faulting within a wedge that accounts for strain of up to 35 mm/yr or (2) a rate of 23 mm/yr elastic slip along the plate interface, resulting in a M8.5 earthquake every century. Since 1964 only one M6.0 event has been recorded along this zone in our catalog. This rate is about $1/10^{th}$ the rate of M6.0 observed farther south in the Northern Sumatra-Andaman section. Applying Gutenberg and Richter (1944) cumulative a- and b-values in Table 1 a M8.5 should occur about every 25,000 yr. For our current model we have applied a Gutenberg-Richter magnitude frequency distribution with parameters set by using the earthquake catalog. This is significantly lower than the rate of earthquakes suggested by Socquet and others (2006).

The Northern Sumatra-Andaman section ruptured in the 2004 Sumatra earthquake M9.2. According to Billam and others (2005) only two additional large earthquakes have ruptured along this zone during the past 200 yr, in 1881 (M7.9) and 1941 (M7.7). About 25 earthquakes greater than M6.0 have occurred during the past century and 11 earthquakes during the past 50 yr yielding a rate of about 0.23 or one event every 4–5 yr. Preliminary paleoseismic data reported in Rajendran and others (2007) indicate that at least one predecessor for the 2004 earthquake occurred 900–1000 yr ago. Based on this paleoseismic data, we have assigned a characteristic M9.2 earthquake to this section of the subduction zone that occurs on average every 1000 yr. Other earthquakes are accounted for by using the historical seismicity to set the rate and b-value for a Gutenberg and Richter (1944) magnitude frequency distribution.

The Sumatra section has been the focus of several large and great earthquakes (fig. 2). Zachariasen and others (1999) studied fossil coral microatolls on the reefs of Sumatra's outer-arc ridge and suggested that the uplift of these reefs is consistent with uplift of about 13 m on the subduction interface. They conclude that this uplift is consistent with M8.8 to M9.2 earthquakes. They prefer a magnitude 9.2 for the 1833 earthquake along that interface and suggest that this would accommodate all of the 49 mm/yr of convergence across the subduction zone. Great earthquakes in 1833 (M8¾) and 1861 (M8¼ to M8½) along the Sumatra subduction zone were also reported by Newcomb and McCann (1987). The Petersen and others (2004) model assumed complete

coupling of 49 mm/yr to obtain a 13 m displacement, resulting in a M9.2 occurring every 265 yr. We have modified this value to allow a 0.8 coupling coefficient, which then results in a M9.2 occurring every 333 yr. We also apply a Gutenberg and Richter (1944) magnitude frequency distribution with parameters obtained from the earthquake catalog. During the writing of this report several large earthquakes ruptured along the Sumatra section of the subduction zone: September 12 M 8.4 and 7.9 and September 20 M 6.9.

The Java section has a high slip rate (60 mm/yr), but publications have questioned how much of this slip is seismic based on the lack of great earthquakes along the interface. For example Pacheco and Sykes (1992) indicated that this zone was fully decoupled. This inference was drawn from the observation that essentially zero seismic moment had been released in the 1900-1990 time span by interface events (see their Table 3). However since that time, M7.7 and M7.8 events have ruptured the interface. Therefore, we have allowed a great M9.2 earthquake to occur in this zone but only use the rate of historical seismicity to constrain the model.

We computed the Gutenberg-Richter a- and b-values from shallow earthquakes that may have occurred on the Java subduction interface ($\hat{a} = 5.78$ (incremental rate of **M** 0 ±0.05) and $\hat{b} = 1.097$). This resulted in a recurrence estimate of 105 yr for M7.7 or greater interface earthquakes, similar to the observed rate of two events during the past 200 yr. This distribution also predicts a mean recurrence time of 5100 yr for M9 events, an interval that is too long to be validated by historical data. Assuming a slip for events of this size we can calculate a seismic slip rate of about 2.5 mm/yr, about 4 percent of the total slip rate along the plate interface.

Crustal Fault Source Models

Long-term slip rates and estimates of earthquake size define the rate of large-magnitude earthquakes on crustal faults in hazard analysis. The length of the mapped fault and downdip width estimates from seismicity may be used to calculate maximum magnitudes of earthquakes expected to occur on these faults (*e.g.*, Wells and Coppersmith, 1994). For determining magnitude from fault area or surface length on different segments or multi-segment ruptures the relations of Wells and Coppersmith (1994) are used.

We also include uncertainty (±M0.2) for the characteristic earthquake magnitude and the maximum magnitude of the Gutenberg-Richter distribution. All of these magnitude-frequency models are moment balanced. To estimate the earthquake recurrence rates on faults, the slip rate is converted to a moment rate and the earthquake magnitude is converted to moment. The ratio of these (the moment rate of the fault and the moment of the rupture) results in the rate of the characteristic earthquake.

We apply a combination of 50-percent characteristic (Schwartz and Coppersmith, 1994) and 50-percent Gutenberg-Richter magnitude frequency distributions and account for uncertainties in the characteristic or maximum magnitudes in the northern southeast Asia faults. In addition, we include an aleatory uncertainty in the magnitude using a normal distribution, with sigma of ±0.12, which was applied in the United States National Seismic Hazard Maps (Frankel and others, 2002). For the Sumatran fault we use an equally weighted combination of two different characteristic models, a Gutenberg and Richter (1944) model, and a floating M7.9 rupture model.

Indonesian Faults

As part of this project we required an inventory of Quaternary faults on the islands of Sumatra and Java and portions of Bali and Kalimantan (west of long. 115° E.). To ensure that we obtained the most complete and current information related to on-land faults in this area, we solicited the support of Dr. Kerry Sieh of the California Institute of Technology (CalTech) and his colleagues at the Indonesian Institute of Sciences (IIS), all of whom have been involved in geological studies of Indonesian faults, deformation, and tectonics for many years.

Within the scope of this work, Dr. Sieh and Dr. Danny Hilman Natawidjaja compiled a geographic information system (GIS) database of active faults and folds in the study area. The compilation relies on publicly released and published information, but in areas where there are obvious, active structures but no published data, they conducted preliminary reconnaissance mapping of landforms that indicate active faulting and tectonics using shaded-relief Shuttle Radar Topography Mission (SRTM) maps and digital topography. In addition, they assembled information on the region's contemporary deformation and a catalog of instrumental and preinstrumental earthquakes from a variety of sources along with topography, published maps, geological features, cultural features, and GPS slip vectors. The fault and fold database (Appendix C) provide a depiction of the geographic and geologic parameters for each structure. Having these various data layers in GIS format allows different sources of information to be merged and visualized together, thereby revealing important spatial relations (*e.g.*, faults can be superimposed on the SRTM topographic base map as in Figure 6).

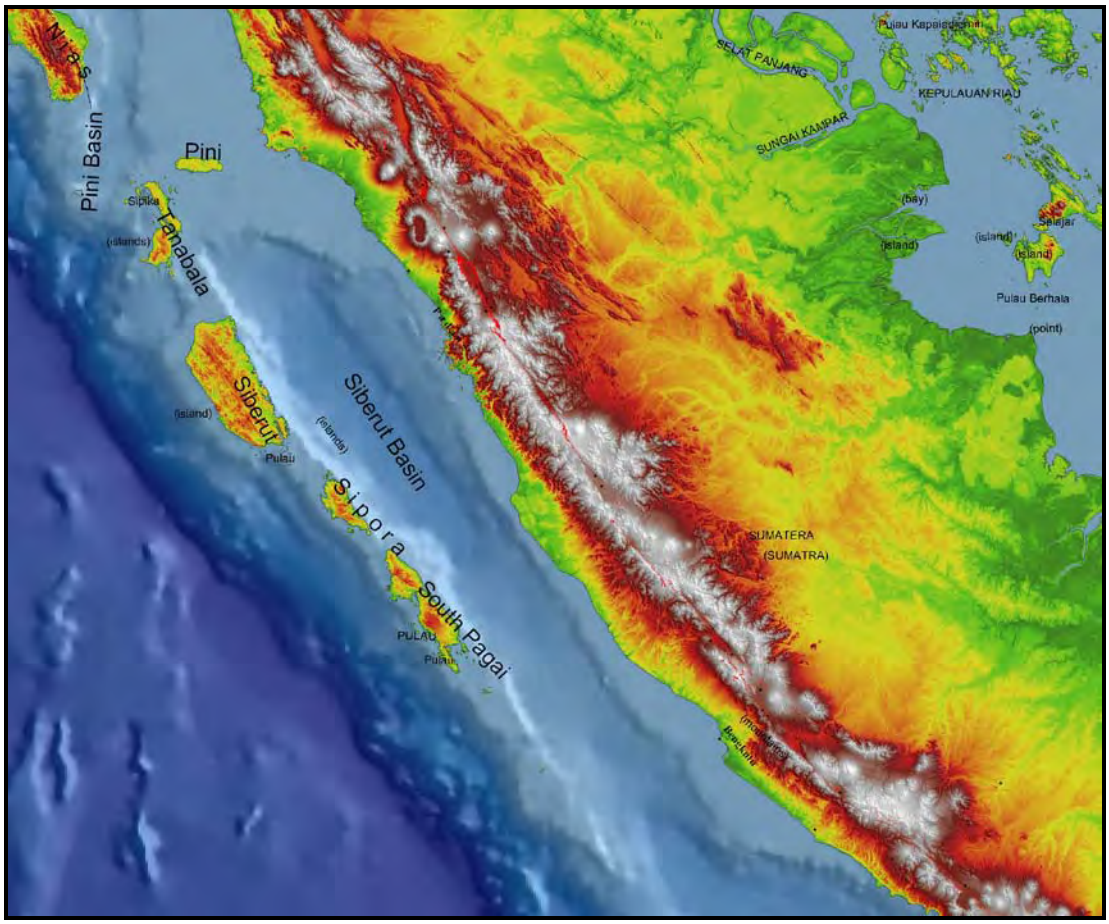

Figure 6. Map showing the Sumatran fault on the island of Sumatra, Indonesia (prepared by Sieh and Natawidjaja, see Appendix B). This figure is associated with a database providing fault parameters.

The Island of Sumatra

The Sumatran fault (fig. 6) is the largest and most prominent on-land structure in the study area. The right-lateral, strike-slip fault extends along the crest of the uplands of Sumatra. Sieh and Natawidjaja (2000) mapped the Sumatran fault zone primarily from 1:100,000-scale aerial photographs and 1:50,000-scale topographic maps, which were detailed enough to identify probable fault segments that can be used for a seismic-hazard evaluation. On the basis of geomorphic and topographic expression of the fault, they divided the fault system into 20 segments that range in length from 35 to 220 km.

In a few locations, geological field relations permit an estimate of the long-term slip rate on the fault system. On the western flank of Kaba volcano, the channel of the Musi River is offset about 600 m in a 60-ka lava flow. This suggests a geological slip rate of about 10 mm/yr. Near the Equator, meanders of the Sianok River channel are offset about 720 m where a deep gorge is cut into a tuff that is about 65 k.y. old, suggesting a geological slip rate of about 11 mm/yr. To the north, several tributaries of the Renun River cut through the 70 k.y. old Toba tuff and are offset dextrally about 2 km, which

indicates a higher slip rate of about 27 mm/yr (Sieh and others, 1991, 1994; Sieh and Natawidjaja, 2000).

GPS data also yield information on fault slip rates at several locations. The GPS slip-rate values range between 23–26 mm/yr, which is significantly larger than some of the geologically determined rates. The reason for differences in the slip rates between these two sources of data is unclear and requires further study.

Historical earthquakes have caused surface rupture on parts of the Sumatran fault system, but the amount of displacement associated with these ruptures is mostly unknown. The two exceptions are the ruptures associated with the 1892 event along the Angkola segment (Muller, 1895; Prawirodirdjo and others, 2000) and the 1926 event along the Sumani segment (Untung and others, 1985; Natawidjaja and others, 1995; Prawirodirdjo and others, 2000).

No site-specific paleoseismological study have been conducted on the Sumatran fault zone, except for the study Bellier and others (1997), who trenched the fault line northwest of Semangko Bay. However, they were not able to determine the dates of and intervals between past ruptures at this site.

The Islands of Java and Bali

A comprehensive search of previous studies and maps of Quaternary faults and folds in Java and Bali yielded no detailed information that was adequate for use in a seismic-hazard assessment. There are a few well-known active faults, including the Cimandiri fault, the Lembang fault, and the Baribis-Citanduy fault zone, but these have been mapped only at regional scales, and the data on these structures are not sufficiently detailed to be useful in modeling seismic hazard. Geologic evidence indicates that these structures are active and therefore, likely pose a seismic hazard, but the level of that hazard cannot be quantified at the present time. This lack of information on known hazardous structures demonstrates the need to study these faults in order to better evaluate the threat that they pose.

Indonesian Kalimantan

The published literature and maps of Indonesian Kalimantan contain no information on Quaternary faults and folds, even on a regional scale. A few significant historical earthquakes have occurred east of long. 115° E., but there has been no significant seismicity west of long. 115° E. We have no geologic or geomorphic information that can contribute to a seismic hazard map for this area.

Sumatran Fault Model

We are only able to characterize the Sumatran fault for the seismic hazard analysis because no fault parameters have been published for any of the other faults in Indonesia. The Sumatran fault is a 1900 km long structure that accommodates right-lateral shear associated with the oblique convergence along the plate margin (fig. 2). This major transverse structure is thought to have ruptured in 1892 in a M7.7 earthquake. The slip rate along the fault is thought to vary from 6–27 mm/yr with the slip rate accelerating to the west (Beaudouin and others, 1995; Sieh and Natawidjaja, 2000). We developed four possible models to account for seismicity on the Sumatran fault (Table 2).

Table 2. Sumatran fault models. Each model is weighted equally.

Model 1			Model 2		
Segment	Slip rate (mm/yr)	Magnitude	Segment	Slip rate (mm/yr)	Magnitude
1	6	7.1	Sunda	11	7.4
2	6	6.8	Semangko	11	7.3
3	8	7.1	Kumering	11	7.6
4	10	7.3	Manna	11	7.3
5	11	7.1	Musi	11	7.2
6	13	7.4	Ketaun	11	7.3
7	15	7.2	Dikit	11	7.3
8	17	7.3	Siulak	11	7.3
9	17	6.9	Suliti	11	7.4
10	23	7.2	Sumani	11	7.1
11	23	7.1	Sianok	11	7.2
12	23	7.5	Sumpur/Barumun	23	7.7
13	23	7.2	Toru	27	7.4
14	23	6.7	Renun	27	7.7
15	23	7.0	Tripa	27	7.7
16	23	7.5	Aceh (south)	27	7.4
			Seulimeum	27	7.5
Model 3			**Model 4**		
Entire fault	17	7.9	Entire fault	17	6.5-7.9

The first model is based on the segmentation model of Beaudouin and others (1995). The slip rates for this model vary from 6 mm/yr to 23 mm/yr. The magnitudes are based on the fault length (Wells and Coppersmith, 1994) and vary from M6.7 to M7.5.

The second model is based on the model of Sieh and Natawidjaja (2000). This model assumes slip rates from 11 mm/yr to 27 mm/yr and the magnitudes derived from the fault length vary from M7.1 to M7.7 (Wells and Coppersmith, 1994).

The third model assumes that M7.9 earthquakes can occur anywhere along the fault. This model is based on an average slip rate of 17 mm/yr rate for the entire fault. We chose the magnitude of 7.9 based on the published magnitude of the 1943 earthquake. The 1943 earthquake has an estimated magnitude 7.6, but the variability inherent in the process of estimating magnitude would allow for a larger magnitude. Therefore, we have increased the magnitude of this earthquake to M7.9 to allow for the possibility that the event was slightly larger than the documented magnitude. In addition, we chose this magnitude because the two largest historical earthquakes on the San Andreas fault in California, which is an analogous strike-slip fault, were about M7.8 and 7.9.

The fourth model is based on a truncated Gutenberg-Richter magnitude frequency distribution (Gutenberg and Richter, 1944) that accounts for a range of different sizes of earthquakes. This model also is based on an average slip rate of 17 mm/yr and assumes a range of magnitudes between M6.5 and M7.9. Each of these models is weighted equally.

Faults in Thailand

Even though no surface-faulting earthquakes have been documented in Thailand in the past 700 yr (Bott and others, 1997; Fenton and others, 1997), wide spread evidence of Holocene surface deformation has been recognized for nearly two decades. These

intraplate faults have tectonic histories that are complex (*i.e.*, Morley, 2002); their origin, distribution, and tectonic history are driven by distant convergent-plate motions. In northern Southeast Asia, a broad zone of generally east-west, sub-parallel, well-defined sinistral faults extend from the Burma coast eastward into Vietnam and China. These faults, join with the Himalayan deformation zone, and define an arc of the India-Asia collision belt. The strike-slip faults of northern and western Thailand give way to transtensional, normal faults in the northeastern corner of the country. The normal faults share striking similarities to faults in the Basin and Range Province of the Western United States (Fenton and others, 1997, 2003). They bound Tertiary basins that reflect similar origin, style of faulting, spatial distribution, and rates of activity as faults in the Basin and Range Province; similarly, northern Thailand is undergoing east-west to northwest-southeast extension (Fenton and others, 1999). Thailand, like vast regions of the Basin and Range, has not had a historic large-magnitude earthquake and therefore is not generally considered seismically active. The geologic record, however, suggests that these generally quiescent faults have been the source of large earthquakes and if earthquake processes are comparable to those in the Basin and Range Province, earthquakes as large as M7.1 (1915 Pleasant Valley, Nevada) to M7.3 (Hebgen Lake, Montana) may occur. The faults we included in our model are long enough to support earthquakes of that size.

There has been an extensive effort in Thailand to document and characterize potentially active faults (Kosuwan and others, 1999, 2000) by the Department of Mineral Resources with cooperative research studies by Chulalongkorn University, Thailand, and Akita University, Japan, that evolved from earlier compilations (Nutalaya, 1994; Hinthong, 1995). In the decade since the earliest of these compilations, many trenching investigations have been completed that identify where large-magnitude Holocene (and earlier) earthquakes have occurred.

We rely on published data to assign slip rates, and our discussions of fault parameters in the Thailand workshops illustrated that published rates vary considerably. This is not a problem unique in Thailand but is recognized worldwide; some (but not all) of the reason for this variation is that relative-dating techniques lack reproducibility. We adopted the strategy to treat each site-specific (trenching) study equally. If the published slip rate is a range of values, we use the average of those end members. Then single-study values are averaged. However, if the result of a study is based on regional comparison of geomorphology and is followed by more recent investigations including trenching, the site-specific studies supercede the regional comparison and the latter was not considered in assigning preferred slip rates.

The earliest and most extensive reconnaissance studies of faults in Thailand are by Fenton and others (1997, 2003). They evaluated the geomorphic expression of faulting; however, the study was handicapped by the absence of a well-defined late Quaternary framework. Because of the regional nature of this study, slip rates were assigned based on broad similarities between faults. We have used their findings in our analysis where they have not been superceded by fault-specific studies. Future work on the Long, Nam Pat, Phayao, and Phrae Basin faults will certainly improve our understanding of these faults. Using the same guiding philosophy, additional sources were characterized by Wong and others (2005). The Khlong Marui fault (fig. 7, Table 3) is generally poorly expressed in the landscape; it is assigned a low slip rate, suggesting

recurrence of M7.5 earthquakes on the order of more than 100 k.y. Likewise the Ranong fault is assigned a slip rate similar to Fenton and others' (2003) low slip-rate faults.

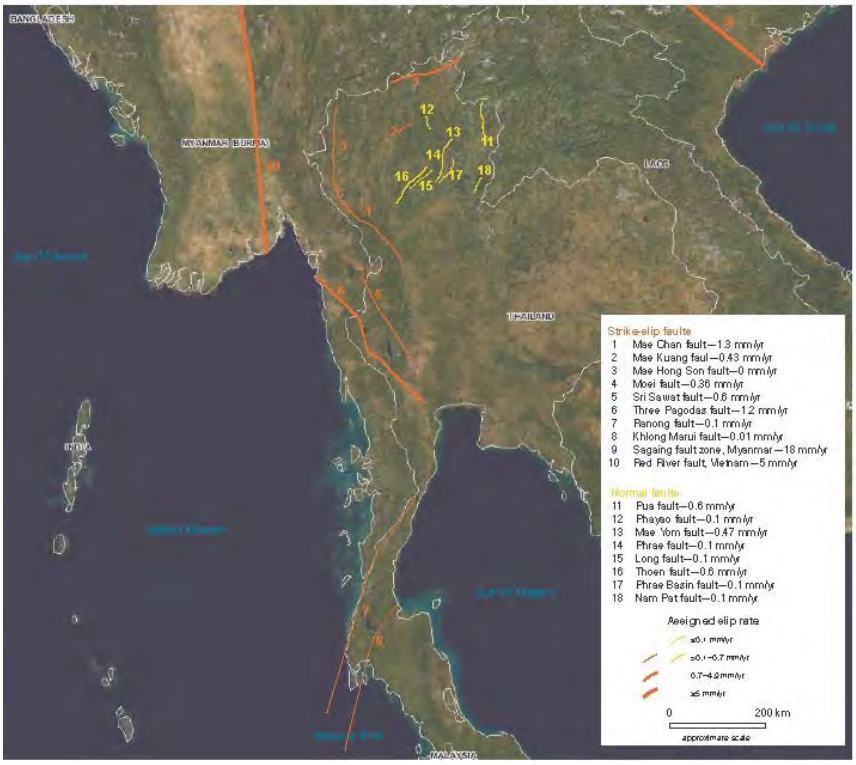

Figure 7. Map of fault sources in and near Thailand.

Table 3. Thailand fault parameters.

Name	Length (km)	Dip (°)	Width	Characteristic M	Slip rate (mm/yr)	Annual probability	Recurrence interval (yr)	Reference
Khlong Marui fault	348	90	15	7.5[1]	0.01	7.8494E-06	127,398	Wong and others, 2005
Long fault	63	50	20	7.17	0.1	6.8464E-05	14,606	Fenton and others, 2003
Mae Chan fault	154	90	15	7.5[1]	0.7	2.4319E-04	4,112	Kosuwan and others, 2003
Mae Kuang fault	34	90	15	6.86	0.43	2.6250E-04	3,809	Rhodes and others, 2004
Mae Yom fault	27	50	20	6.74	0.47	7.6717E-04	1,303	Charusiri and others, 2006
Moei fault	226	90	15	7.5[1]	0.36	1.8383E-04	5,439	Saithong and others, 2005
Nam Pat fault	38	50	20	6.91	0.1	1.1574E-04	8,640	Fenton and others, 2003
Phayao fault	30	50	20	6.80	0.1	1.3075E-04	7,648	Fenton and others, 2003
Phrae Basin fault	65	50	20	7.18	0.1	6.9868E-05	14,312	Fenton and others, 2003
Phrae fault	73	50	20	7.24	0.06	4.7533E-05	21,037	Udchachun and others, 2005
Pua fault	80	50	20	7.29	0.6	3.6844E-04	2,714	Fenton and others, 2003
Ranong fault	523	90	15	7.5[1]	0.1	1.x1801E-04	8,473	Wong and others, 2005
Sri Sawat fault	209	90	15	7.5[1]	0.6	2.8216E-04	3,544	Kosuwan and others, 2006
Thoen fault	107	50	20	7.43	0.16	9.2634E-05	10,795	Charusiri and others, 2004 Pailoplee, 2004
Three Pagodas fault	380	90	15	7.5[1]	0.56	4.7944E-04	2,085	Charusiri and others, 2004 Kosuwan and others, 2006

[1] Characteristic magnitude fixed based on worldwide analog.

The other faults in our analysis have been targets of more recent detailed paleoseismological investigations. These fault parameters were discussed at the Thailand workshops and represent the best assessment at this time. We will provide only brief remarks regarding these faults that are relevant to seismic hazard mapping. Refer to Figure 7 and Table 3.

The Mae Chan fault is an east-west left-lateral strike slip fault in northern Thailand, located near the city of Mae Chan. It extends from near the Myanmar border in the Nam Mae Kok valley eastward into Laos across the Mekong River (Fenton and others, 2003). The morphology of the Mae Chan fault demonstrates clear evidence of late Quaternary surface faulting including such features as shutter ridges, sag ponds, and beheaded gullies (Wood, 1995, 2001, Hinthong, 1995; Rymer and others, 1997). Long-term activity is evident in satellite imagery showing offset, on the scale of hundreds of meters, of active river channels. Based on assumed erosions rates Fenton and others (2003) suggest that the Mae Chan fault has a slip rate of 0.3–3 mm/yr. More recent trenching by Kosuwan and others (2003) suggest a lower slip rate of 0.7 mm/yr with possibly three surface-rupturing events occurring in the Holocene. Our assigned slip rate is based on the more recent and detailed study.

The Mae Kuang fault was first reported by Perez and others (1999) as a 30-km-long fault subparallel to and south of the Mae Chan fault and northeast of the Chain Mai basin in the Mae Tho Range. It, like the Mae Chan fault, is a strike-slip structure. Our assigned slip rate is the average of long-term rates proposed by Rhodes and others (2003) of between 0.175 and 0.7 mm/yr based on 3.5 km offset since the reversal of faulting between 5 and 20 Ma.

The Mae Yom fault strikes northeast for a distance of approximately 25 km. Recent investigations suggest multiple Holocene displacements with the most recent movement about 5 k.y. ago (Charusiri and others, 2006).

The predominately strike slip, nearly 230-km-long Moei (or Mae Ping) fault trends northwest near and paralleling the western border of Thailand. Recent studies of this fault suggest recurrence intervals measured in tens of thousands of years and a slip rate of 0.36 mm/yr (Saithong and others,2005).

The fault with the lowest slip rate assigned in this model is the centrally located Phrae fault. The assigned slip rate is from Udchachun and others (2005). However, previously published slip rate of 0.1 mm/yr (Fenton and others, 2003) is based on regional similarities, but the basis of this slip rate is not documented. Our model suggests recurrence intervals on the order of tens of thousands of years.

The Pua fault, in the northeasternmost part of Thailand, demonstrates unmistakable evidence of recurrent and recent faulting. The range-front is abrupt and linear in satellite imagery clearly highlighting this west-dipping normal fault. Fenton and others (2003) document that the youngest and best-expressed geomorphology is found along the northern and central part of the fault. They assign a slip rate of 0.6 mm/yr to this fault based on comparative geomorphology. A more recent study by Charusiri and others (2006) does not document a slip rate for this fault, but trenching suggests that surface rupturing earthquakes have occurred 8,000, 6,000, and 2,800 yr ago. The annual rate of 3.184E-04 from our study is in agreement with the chronology documented by Charusiri and others (2006).

The west-dipping, normal Thoen fault (Fenton and others, 2003) bounds the eastern side of the Thoen, Mae Moh and Lampang basins. Recurrent activity along this fault has resulted in a series of faceted spurs reaching 250 to 350 m in height and deeply entrenched wine-glass valleys. The range front is abrupt in satellite imagery, which provides further evidence that this fault has been the source of recurrent large magnitude earthquakes. Fenton and others (2003) document 6 m offset of the active floodplain of the Mae Mai River. The absolute age of this terrace surface was not determined, but its assigned age is 10 ka. There is a general lack of wide-spread evidence of Holocene offset; therefore, the actual slip rate may be much lower as documented by later studies by Charusiri and others (2004) and Pailplee (2004) who conclude that the slip rate is 0.15 mm/yr and 0.17 mm/yr, respectively. The assigned slip rate is the average of the most recently published rates.

The Sri Sawat and Three Pagodas faults are subparallel, strike-slip faults that have similar slip rates in our model. Fault parameters are poorly known and recent studies do not concur. Fenton and others (2003) suggest a broad range of 0.5-2 mm/yr for the Three Pagodas fault based on geomorphic input and relative dating techniques. Later studies suggest slip rates of 0.22–0.5 mm/yr (Charusiri and others, 2004) and 0.76 mm/yr (Kosuwan and others, 2006); these are the basis of our assigned slip rate. The Three Pagodas fault is especially important because it is the primary contributor to hazard in Bangkok, Thailand, because this source is closest to the city. The assigned slip rate for the Sri Sawat fault is based on studies by Kosuwan and others (2006). Their study indicates that at least one large-magnitude Holocene earthquake has occurred on this fault.

In addition to location and slip rate, the third dimension of fault sources must also be defined. Bott and others (1977) provide a summary of seismicity in Thailand that indicates that the majority of seismicity occurs at depths of 10–20 km. Therefore, we assign an average depth (15 km). The assigned dip for the normal faults in our model reflect the default value used in the United States. All slip rates are either vertical, for normal faults, or horizontal, for strike-slip faults; therefore, the fault parallel widths (20 km) are larger on dipping faults than similar strike-slip faults. The long faults in the model (> 90 km) are assigned maximum magnitudes of M7.5 based on world-wide analogs.

Other Regional Sources

Most of the Thailand faults in our model have characteristic magnitudes with recurrence times of several thousands of years. Earthquake hazard can be influenced by faults and sources in neighboring countries; therefore, a literature search was conducted to evaluate any significant seismic sources beyond the borders of Thailand. Two faults have recurrence intervals on the order of a few hundred years: The Red River and Sagaing faults (fig. 7, Table 4). These faults cause the highest hazards in the northern portion of Southeast Asia.

The Sagaing fault in Myanmar is a major right-lateral strike-slip fault that carries some or all of the oblique plate motion related to the India-Eurasian convergence similar to the Sumatran fault on the island of Sumatra. Our assigned slip rate is based on high rates of strain accumulation suggested by GPS studies (Socquet and others 2006). Socquet and others (2006) indicate that the GPS rate is similar to rates documented in

earlier geologic studies (Bertrand and others, 1998). Like the Sumatran fault we modeled the Sagaing fault with floating M7.9 earthquakes that have equal probability of rupturing along the fault.

The other source, the Red River fault in Vietnam and China (fig. 7, Table 4), is another major, long (>900 km) right-lateral strike-slip fault. Reported slip rates are 2-8 mm/yr (Allen and others, 1984) based on measured offsets between 9 m and 6 km; the average was used in this model, which agrees with data presented by (Replumaz and others, 2001; Schoenbohm and others, 2006). The slip rate of the Red River fault is poorly constrained because of the lack of radiometric age dating of offset landforms. Like the Sagaing fault, we constrain the maximum magnitude at M7.9.

Table 4. Regional fault parameters.

Name	Length (km)	Dip (°)	Width	Characteristic M	Slip rate (mm/yr)	Annual probability	Recurrence interval (yr)
Red River fault	890	90	15	7.9[1]	5		
Sagaing fault zone	724	90	15	7.9[1]	18	7.3877E-03	135

[1] Characteristic magnitude fixed based on worldwide analog.

Ground Motion Models

The ground motion models are referred to as attenuation relations or ground motion prediction equations. These models predict the ground motion for a particular fault source, fault type, magnitude, distance, stress drop, Q attenuation properties of the crust, and local soil condition. We apply attenuation relations for intraplate earthquakes within stable continental regions, interplate crustal earthquakes near plate boundaries, subduction zone earthquakes on the plate interface, as well as intermediate and deep earthquakes within the subducting slab.

Crustal Intraplate Attenuation Relations

Once the earthquake sources are defined, attenuation relations relate the source characteristics of the earthquake and propagation path of the seismic waves to the ground motion at a site. Predicted ground motions are typically quantified in terms of a median value (a function of magnitude, distance, site condition, and other factors) and a probability density function of peak horizontal ground acceleration or spectral accelerations for different periods (McGuire, 2004). We apply separate attenuation relations for the interplate crustal, intraplate crustal, deep, and subduction earthquakes. Ground motion maps are produced by considering the ground motion distributions from each of the potential earthquakes that will affect the site and by calculating the ground motion with an annual rate of 1/475 or 1/2475 (10% and 2% probability of exceedance in 50 yr) for building code applications.

For the stable Sunda plate we use the crustal intraplate attenuation relations to characterize the ground motions. We have applied the following weighting scheme for these attenuation models: Toro and others (2005; wt. 0.2), Frankel and others (1996; wt. 0.1), Atkinson and Boore 140 bar stress drop (2006, 2007; wt. 0.1), Atkinson and Boore 200 bar stress drop (2006, 2007; wt .0.1), Somerville and others (2001; wt. 0.2), Campbell (2002; wt. 0.1), Tavakoli and Pezeshk (2005; wt. 0.1), and Silva and others

(2005, wt. 0.1). These models account for variable stress drops, finite faults, and cratonic attenuation properties.

The Southeast Asia seismic hazard maps are made using a reference site condition that is specified to be the boundary between NEHRP classes B and C, with an average shear-wave velocity in the upper 30 m of the crust of 760 m/s (Building Seismic Safety Council, 2003). However, some attenuation relations are not developed for this shear-wave velocity. Therefore, for the intraplate attenuation relations we have typically converted hard-rock attenuation relations to approximate ground motions for a site with shear velocity on the NEHRP B/C boundary. For several of these models the hard rock (NEHRP A) to firm rock (NEHRP – BC) conversion that we used for these maps is a simple factor for many spectral periods. These factors are: 1.74 for 0.1 s, 1.72 for 0.3 s, 1.58 for 0.5 s, and 1.20 for 2.0 s spectral acceleration (SA). Similar factors are available for PGA, 0.2 s, and 1.0 s.

Another parameter that is important in ground motion simulations for the intraplate attenuation relations is stress drop, or the compactness of the earthquake rupture. Based on the recommendation of G. Atkinson, we have applied two alternative stress drops of 140 bars and 200 bars for the Atkinson and Boore (2006, 2007) model to account for epistemic uncertainty in that parameter.

Crustal Interplate Attenuation Relations

For this hazard analysis, we apply the crustal interplate attenuation relations to all crustal faults in Thailand and Indonesia. There was some discussion about whether the faults in Thailand should be treated as intraplate events since the ground motions may persist to longer distances as they propagate into a region of lower attenuation. This issue was unresolved at our workshops and should be a topic of future studies to improve the maps.

Research sponsored by the Pacific Earthquake Engineering Research Center (PEER) and involved in the Next Generation Attenuation Relation project (NGA) developed a global strong motion database containing strong motion records from 173 earthquakes. These data were used to revise crustal ground motion prediction equations between 2002 and 2006. The goals of the each of the NGA modelers was to apply their own selection criteria to the database but justifying why data was discarded and documenting why different choices were made in developing the models. In addition, the modelers used 1-d simulations of rock ground motions, 1-d simulations of shallow site response, and 3-d simulations of basin response to constrain their models.

The attenuation relations used in this update of the hazard maps were posted on the PEER website on January 19, 2007. The USGS sponsored a workshop on NGA equations that gave the external community an opportunity to comment on the equations (October 2005) and we convened an expert panel on strong ground motion models to provide advise on how to implement the NGA equations in the national maps (September 2006). This panel recommended that we include three NGA attenuation models for calculating ground motions from crustal Western United States earthquake sources: Boore and Atkinson (2007), Campbell and Bozorgnia (2007), and Chiou and Youngs (2007). The new ground motions saturate at large magnitudes and give lower ground motions for all magnitudes at source-receiver distances between 10 and 50 km. We assign

equal weights to each of the three NGA equations based on recommendations from the expert panel on ground motions.

Subduction Zone Attenuation Relations

In the United States, ground motions for great Cascadia earthquakes were determined from: Youngs and others (1997, wt. 0.25), Atkinson and Boore (2003; global model, wt. 0.25), and Zhao and others (1997, wt. 0.5). The Zhao and others (1997) relation predicts higher ground motions closer to the fault source than the other two relations. This difference results in an increase in the hazard compared with the earlier model of Petersen and others (2004).

Intermediate Depth Attenuation Relations

To calculate ground motions for intermediate depth earthquakes (>40 km), we used the attenuation relation by Geomatrix Consultants (1993) with modification for depth dependence that was incorporated in the 1996 and 2002 United States national seismic hazard maps. In addition we included the Atkinson and Boore (2003) equations for intraslab earthquakes. Deep events were assumed to occur at various depths (Table 1: 0-50 km, 50-100 km, 150-200 km, and 200-250 km) for the ground motion calculations.

Southeast Asia Risk Model (example for Padang, Indonesia)

The risk model for Padang, Indonesia, is based on the seismic hazard model described in the previous sections, and the soils/velocity model and fragility model described below. The hazard in the previous section is developed for a uniform site condition of an average shear wave velocity in the upper 30 m (Vs30=760 m/s). In this section, the hazard is developed for the soil conditions on the velocity map described below, in order to obtain more realistic hazard values. These hazard results with amplification for site conditions included are coupled with a hypothetical fragility relation for building construction to demonstrate the development of a collapse risk map.

Shear-Wave Velocity Map for Padang, Indonesia

For the Padang region of Sumatra, we generated a preliminary map of estimated shear-wave velocities for the upper 30 m of the subsurface, Vs30. An estimated shear-wave velocity map such as this is one simple way to characterize varying site conditions, and it can also be used to model earthquake-related ground shaking (*e.g.*, Petersen and others, 1997; 1999; Wills and others, 2000). Furthermore, results from ground shaking modeling can also be used with other data, such as population data, to model associated seismic risks.

This preliminary Vs30 map for the Padang region covers an area of about 18,000 km^2, an area that includes the densely populated metropolitan area of Padang as well as areas of significant population and infrastructure in a much larger region surrounding Padang. This preliminary Vs30 map is based on 1:250,000-scale geologic maps that were published by the Geological Survey of Indonesia during the mid 1970s (Kastowo and Gerhard, 1973; Silitonga and Kastowo, 1975; Rosidi and others, 1976) and a comparison of geologic units described in those geologic map publications with geologic units in California that are discussed and assigned Vs30 velocity ranges in previous studies there (*e.g.*, Petersen and others, 1997; 1999; Wills and others 2000).

Those previous Vs30 assignments and maps for California are in part constrained by field observations and by actual measurements of shear-wave velocities in numerous geologic units of California. This map and characterization of shear-wave velocities for near-surface geologic units underlying the Padang region lacks the constraints that those observations and measurements provided the California Vs30 investigations. With that inherent uncertainty and limitation noted for this preliminary Vs30 map of the Padang region, the techniques used to create the Padang region Vs30 map are briefly discussed below.

To produce the Vs30 map for the Padang region we initially (1) acquired the three 1:250,000-scale geologic maps cited above, (2) scanned the maps, and then (3) rectified and digitized all or parts of these individual maps in GIS. Of the region covered by these three 1:250,000-scale maps, we selected an area of about 18,000 km^2 (fig. 8), based partly on population density and based partly on time limitations for this effort. As such, this area does not include all of two of the geologic maps, which are shown scanned and rectified in Figure 9, but it does include a relatively large and relatively densely populated region of Sumatra that straddles the Sumatra fault zone. With the exception of a few geologic map units of very limited extent (*e.g.*, map units less than about 1 km^2 in area), all geologic units shown on the geologic maps in the area selected (fig. 9) were initially digitized and assigned the map unit labels shown on the original geologic maps. The digitizing of the geologic maps was by far the most time consuming part of this effort and it should be noted that the existence of previously digitized geologic maps would greatly reduce the effort required.

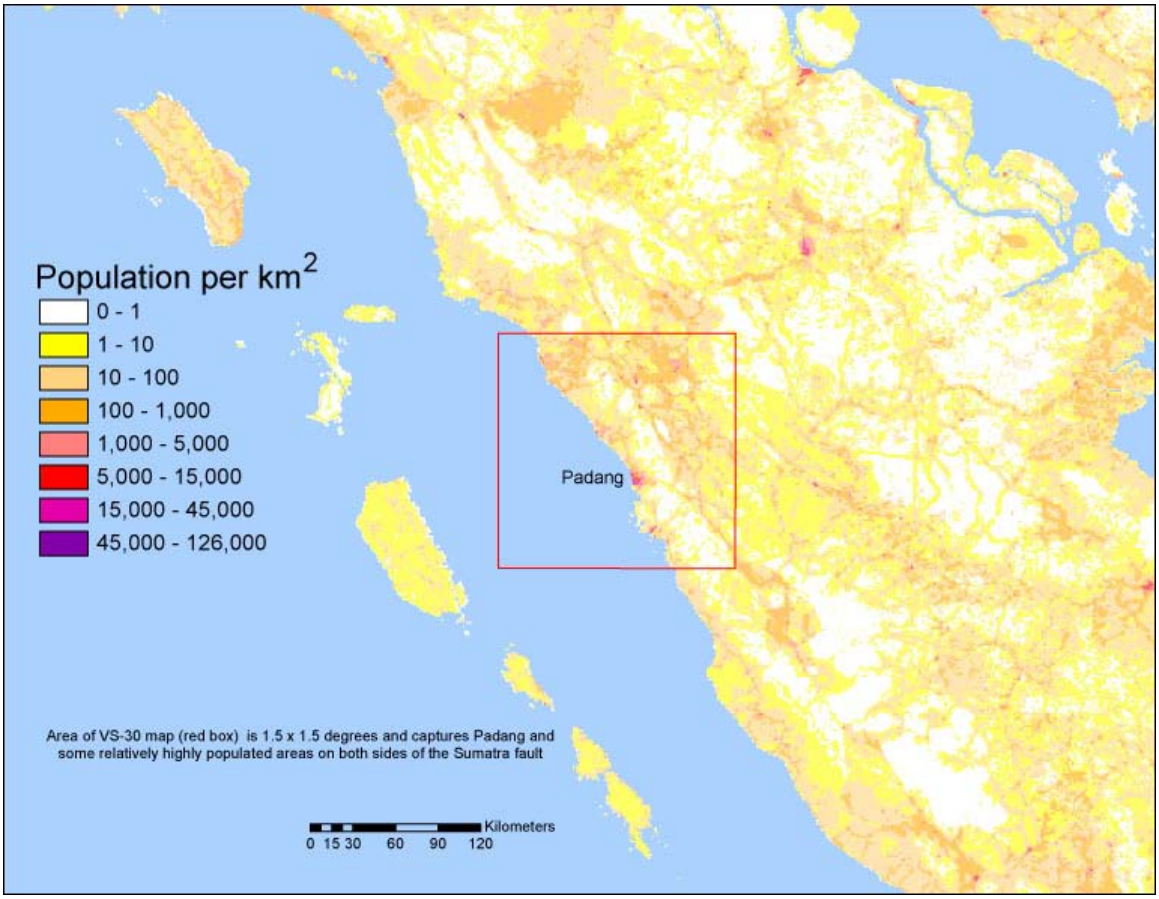

Figure 8. Map showing area of study area (red box) for the preliminary Vs30 map of the Padang region. Map covers about 18,000 km^2 of Sumatra and includes the densely populated metropolitan region of Padang, as well as areas of significant population and infrastructure in a much larger region surrounding Padang. The 2004 population density data shown here is from Oak Ridge National Laboratory (Landscan™ Global Population Database, 2004).

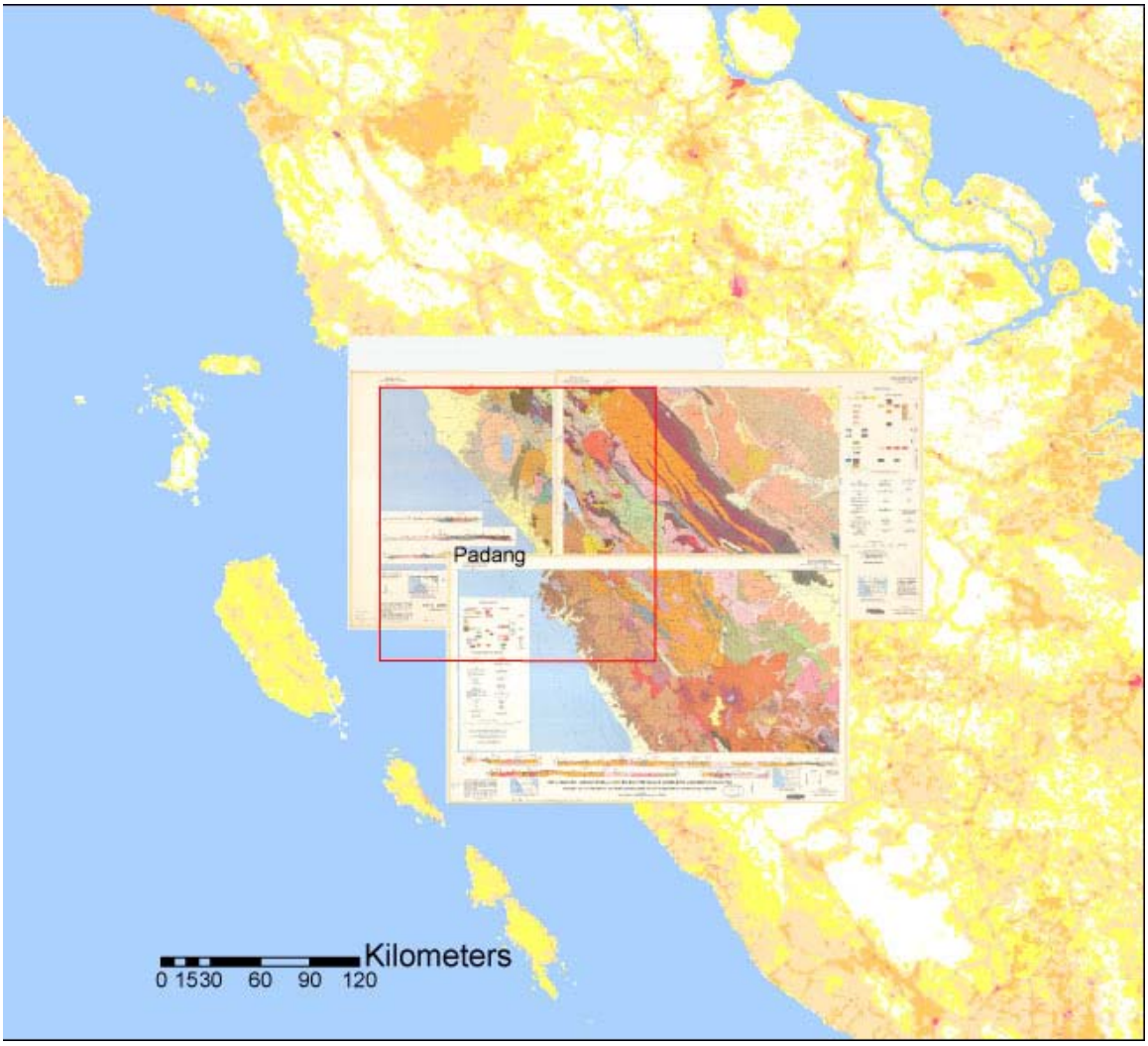

Figure 9. Map showing the three 1:250,000-scale geologic maps that were used as the basis for the shear-wave velocity (Vs30) characterization of the Padang region (red box). Maps are shown after scanning and rectifying these maps in GIS (see text).

After digitizing the geologic map data, the following iterative steps were then used to assign Vs30 values to the digitized geologic units. First we essentially evaluated the character of the individual geologic units based on the descriptions of these units that accompanied the published geologic maps. During that evaluation, we lumped many of geologic map units based on their apparently similar lithologic, hardness, and/or age characteristics. As a result of that lumping of the geologic units, we produced a generalized geologic map of this region (fig. 10). This generalized geologic map lumps geologic units that we determined would likely have similar Vs30 values. We then compared the characteristics of the generalized geologic units to geologic units of California that are discussed and assigned Vs30 ranges in Petersen and others (1999) and Wills and others (2000). Tables 5 and 6 briefly summarize this final comparison and assignment of Vs30 values to the generalized geologic units of the Padang region. The original geologic unit descriptions for the Padang region that were used as a source for

information regarding their physical properties are published with the original 1:250,000 scale maps, and hence that descriptive information is not provided here.

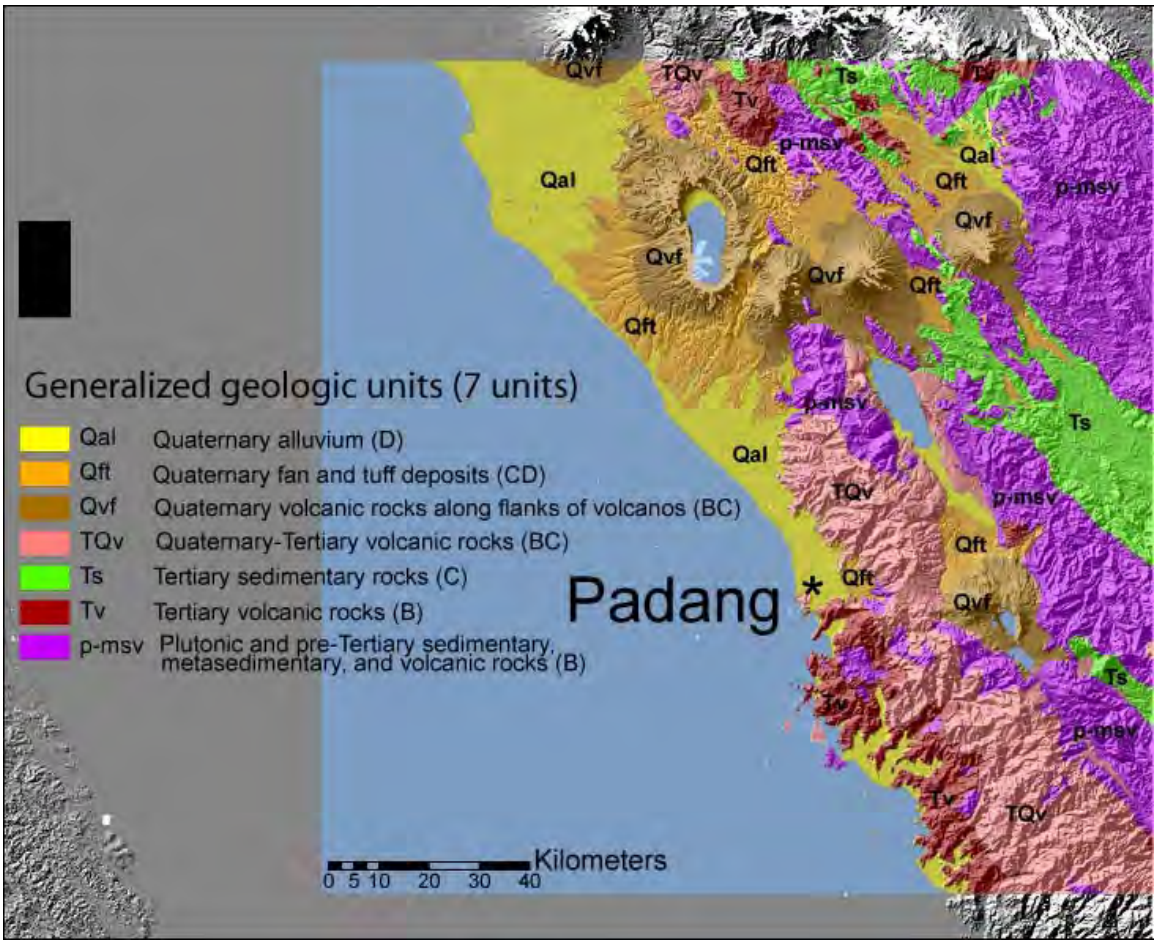

Figure 10. Map showing generalized geologic units of the Padang region, which was created by grouping the numerous geologic units shown on the three original 1:250,000-scale geologic maps in fig. 9. Generalization was based on inferred similarity in physical properties (*e.g.*, hardness). The Vs30 assignments shown on the Vs30 map in fig. 11 are also shown here in parentheses.

Table 5. Vs30 assignments for California geologic units (Wills and others, 2000).

Vs30 category	Expected Vs30 Range (m/sec)	Description of geologic units.
B	>760	Plutonic and metamorphic rocks, most volcanic rocks, coarse sedimentary rocks Cretaceous or older in age.
BC	555-1000	Franciscan Complex rocks except "mélange" and serpentine, crystalline rocks of the Transverse ranges which tend to be more sheared, and Cretaceous siltstones or mudstones.
C	360-760	Franciscan mélange and serpentine, sedimentary rocks of Oligocene to Cretaceous age, or coarse-grained sedimentary rocks of younger age.
CD	270-555	Sedimentary rocks of Miocene and younger age, unless formation is notably coarse grained, Plio-Pleistocene alluvial units, older Pleistocene alluvium, some areas of coarse younger alluvium.
D	180-360	Younger (Holocene) alluvium.
DE	90-270	Fill over bay mud in the San Francisco Bay Area, fine-grained alluvial and estuarine deposits elsewhere along the coast.
E	<180	Bay mud and similar intertidal mud.

Table is summarized and modified from information on p. S190 and Table 3 in Wills and others (2000).

Table 6. Vs30 assignments for Padang region geologic units (7 units).

Vs30 category	Description of geologic units
B	p-msv -- Plutonic and pre-Tertiary sedimentary, metasedimentary, and volcanic rocks
B	Tv -- Tertiary volcanic rocks
BC	TQv -- Quaternary-Tertiary volcanic rocks
BC	Qvf --Quaternary-Tertiary volcanic rocks
C	Ts -- Tertiary sedimentary rocks
CD	Qft -- Quaternary fan and tuff deposits
D	Qal -- Quaternary alluvium (includes some swamps, bay and estuary mud)

As a final step, the Vs30 categories assigned to our generalized geologic units were used to generate a Vs30 map (fig. 11). As indicated in Table 6, some of the generalized geologic map units were assigned to the same Vs30 categories and this effectively reduced the number of Vs30 map units to five from the seven generalized geologic map units. It should be noted that Petersen and others (1999) and Wills and others (2000) included the shear-wave velocity categories of DE and E (see Table 5) for geologic materials such as intertidal and bay mud. Although similar mud probably underlies some coastal areas of the Padang region, the small-scale geologic maps used for this study did not consistently distinguish coastal mud-rich units from alluvium (Qal). Consequently mud-rich units and the Vs30 categories DE and E to which these units are commonly assigned do not exist on the generalized geologic and Vs30 maps for the Padang region (figs. 10 and 11).

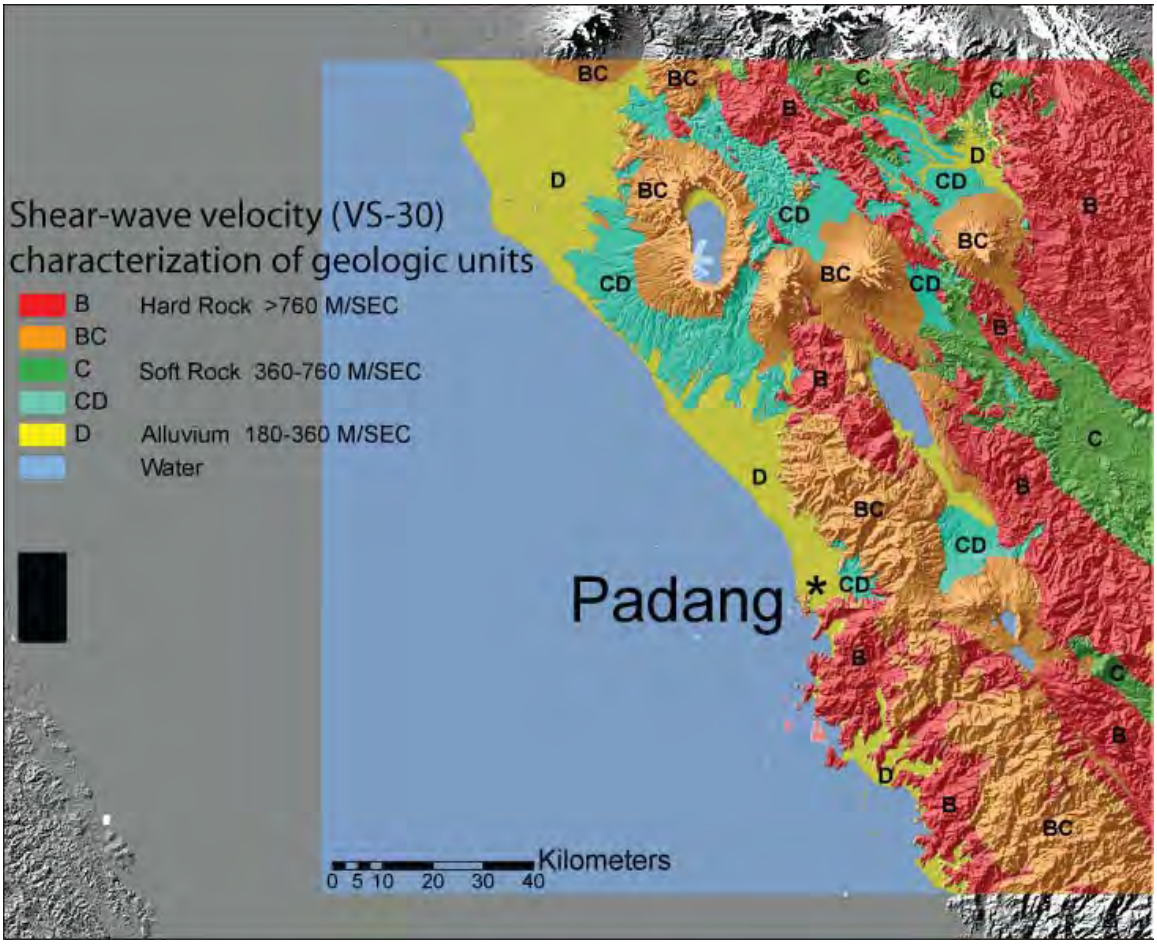

Figure 11. Map showing the shear-wave velocity (Vs30) site characterization for the Padang region. Map was derived by assigning shear-wave velocitt categories to the generalized geologic units shown in Figure 10 (also see table 6).

In order to portray the distribution of the mapped Vs30 units relative to the distribution of population in the Padang region, we also obtained population data for this region. Figure 12 shows the outlines of the mapped Vs30 units overlain on a 2004 population map obtained from Oak Ridge National Laboratory (Landscan™ Global Population Database, 2004). Both the site characterization data provided by the Vs30 map and the population density data shown in Figure 12 were converted to gridded data for use in modeling ground shaking hazard and risk, as presented below.

We amplified the firm rock (Vs 70 m/s) hazard map using using the Vs30 characterization along with the NEHRP (1997) factors to obtain a map that includes soil effects. These hazard values are applied to the risk analysis for Padang.

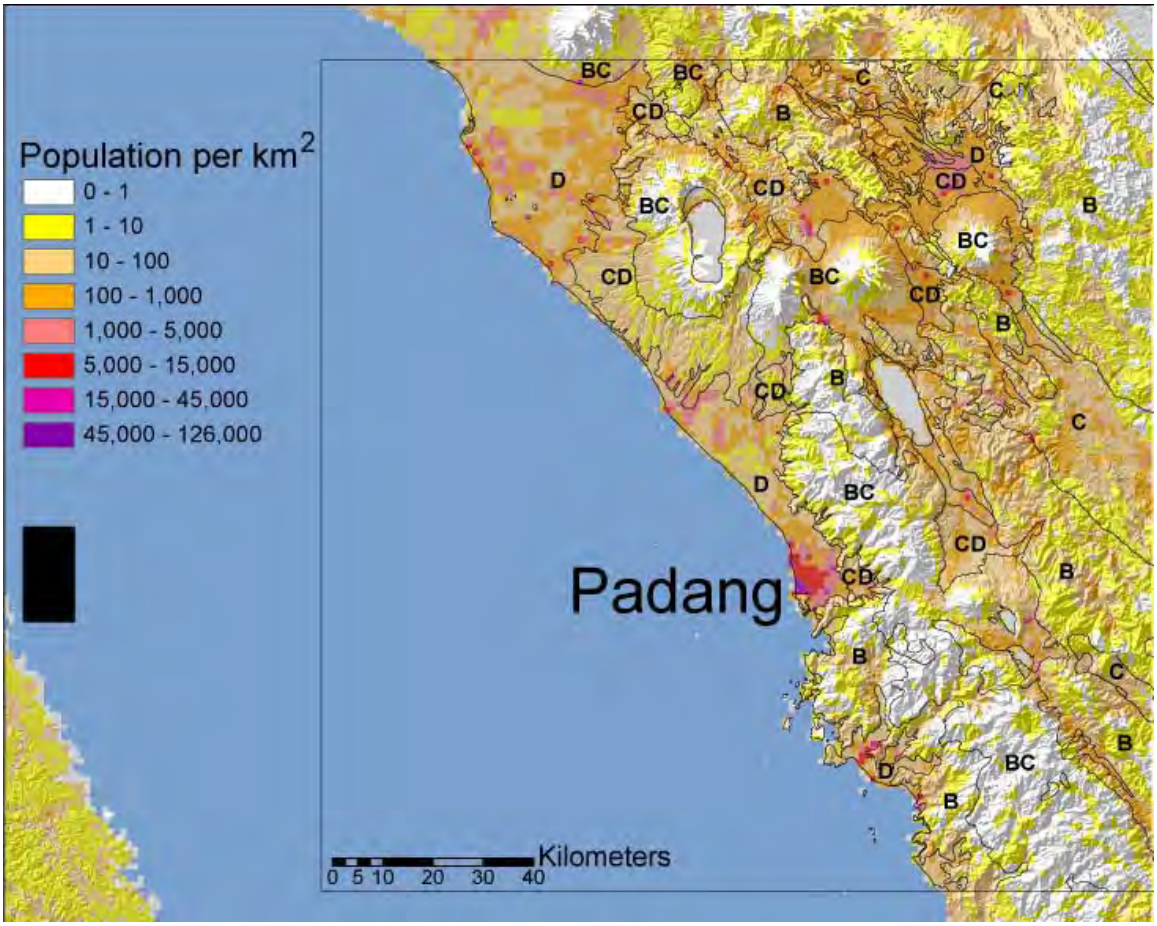

Figure 12. Map showing outlines and labels for the Vs30 units, which are also shown in Figure 10, overlain on a population-density map derived from data obtained from Oak National Laboratory (Landscan™ Global Population Database, 2004).

Risk Map for Padang, Indonesia

The risk map provided in this section for demonstration purposes makes use of hazard curves like those shown in Figures 15 and 16 (below). Unlike the hazard curves shown there, though, the hazard curves utilized here are for the shear wave velocities (Vs30's) shown in Figure 11 (above). One such hazard curve at each point on a 0.01-degree grid covering the Padang region is used in the so-called risk integral (e.g., McGuire, 2004), expressed in Equation 1, to calculate the mean annual frequency of collapse of a building hypothetically located at each grid point. The risk map in Figure 13 displays these results.

$$P_f = \int_0^\infty P_f(a) \left| \frac{\mathrm{d}H(a)}{\mathrm{d}a} \right| \mathrm{d}a \qquad (1)$$

In Equation 1, P_f denotes the mean annual frequency of collapse of the building, $H(a)$ denotes the hazard curve for the grid point location, and $P_f(a)$ denotes the fragility model for the building. The fragility model provides the probability of collapse under a ground motion spectral acceleration equal to a.

The fragility model used to create (via Equation 1) the risk map in Figure 13 assumes a 10% probability of collapse under a 0.2-second spectral acceleration of 1g. The probabilities of collapse at other ground motion levels are assumed to follow a lognormal cumulative distribution function with logarithmic (base e) standard deviation 0.8. According to recent results from the Applied Technology Council ATC-63 Project (personal communication, Dr. Charles A. Kircher, 2007), this assumed fragility is on average consistent with that of low-rise buildings (approximately 2 stories in height) designed in accordance with the present *NEHRP Recommend Provisions for Seismic Regulations for New Buildings and Other Structures* (in preparation) for a ground motion level roughly corresponding to that expected in the *Uniform Building Code* (e.g., 1997) Seismic Zone 4.

Since it is unlikely that existing low-rise buildings in the Padang region are designed to the relatively stringent requirements just described, the annual frequencies of collapse on the risk map in Figure 13 (based on the hypothetical fragility model) can be considered as lower bounds. If the *International Building Code* were adopted in Indonesia, the risk map provided would be reasonably representative for newly-constructed low-rise buildings. Regardless, the observed trends towards relatively large annual frequencies of collapse, or risk levels, along the Sumatran Fault and on softer soils (e.g., Vs30 category D) are informative. Furthermore, the quantification of risk can serve to motivate mitigation measures and provide a basis for prioritization.

If in the future fragility models specific to Indonesian construction are developed (which was beyond the scope of this hazard-focused project), the procedure for developing risk maps that has been demonstrated here can be followed to arrive more region-specific (and likely building-type-specific) risk results.

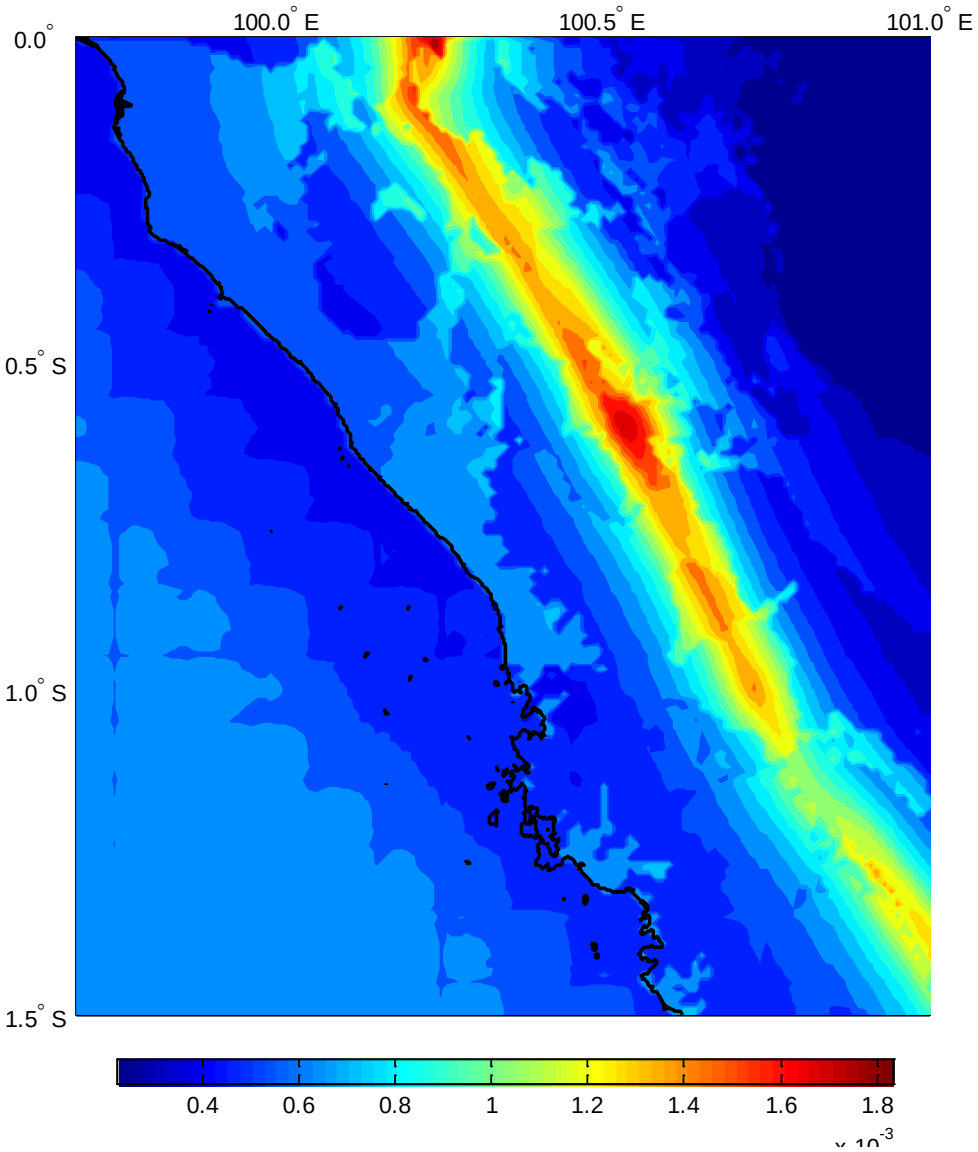

Figure 13. Example risk map for the Padang region showing the annual frequency of collapse of a generic low-rise building hypothetically located at each point on the map. Because of the assumed fragility model, developed merely for demonstration purposes, the mapped values can be considered as lower-bound estimates of the risk.

Results

We have calculated the hazard in Sumatra and Java Indonesia, Malaysia, and Thailand. Plate 1 shows the hazard map for the peak ground acceleration at a 10-percent probability of exceedance in 50-yr hazard level and firm rock site condition (Vs30=760 m/s). Appendix C and D show the 2% and 10% probability of exceedance in 50 year

hazard for peak ground acceleration and spectral accelerations at 0.2 and 1 s on firm rock site condition. The hazard is highest over the Sunda subduction zone, the Sumatran fault, and Sagaing fault (in Myanmar), and the Red River fault (in northern Vietnam).

Indonesia

Seismic hazard on the islands of Java is controlled by three categories of sources in the USGS model, (1), shallow background seismicity, (2) deep (intraplate) background seismicity, and (3) subduction, of which Sumba Java is the nearest and most important. Fault hazard on these islands has not yet been incorporated into the USGS model (Aug 2007). The next figure (fig. 15) shows the relative contributions of these three sources, along with the more distant but more frequent Sumatra subduction zone earthquakes, to a site in Jakarta, Indonesia. The X-axis corresponds to 1-Hz Spectral Acceleration, and the Y-axis to mean annual frequency of exceedance. The graphs in this figure show that for Jakarta, seismic hazard is dominated by shallow crustal seismicity (red curve) and deep interface seismicity (black curve), rather than by interface earthquakes (green and yellow curves, respectively). Comparing the green and yellow curves, we see that Sumatra **M**9.2 subduction events with recurrence of about 333 yr contributes about the same hazard in Jakarta as Java-Sumba subduction events (with much longer recurrence at large M) for 1-s spectral acceleration greater than 0.1 *g*.

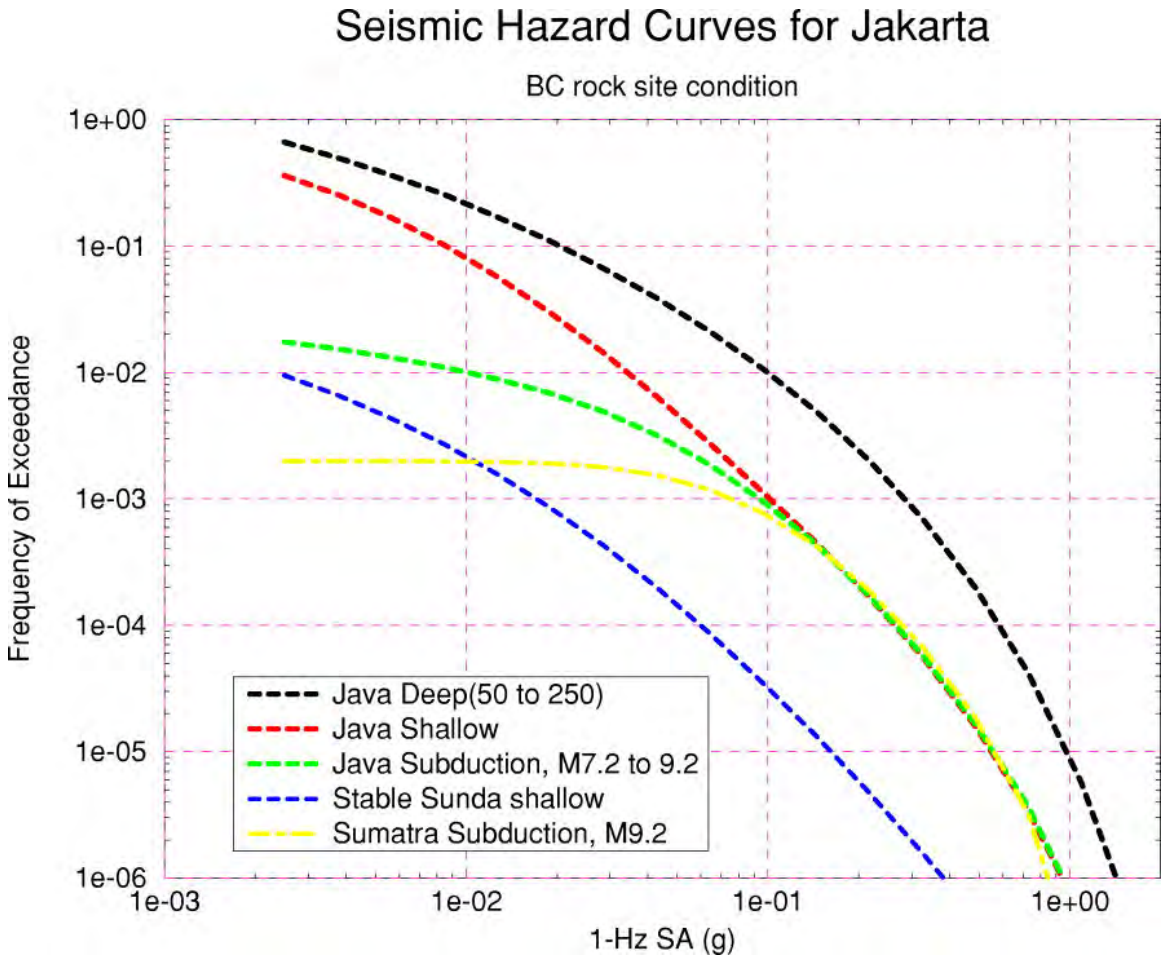

Figure 15. Hazard curves for 1-Hz spectral acceleration at a site in Jakarta, Indonesia.

Thailand

Seismic hazard in Thailand tends to be controlled by subduction and deep seismicity at coastal sites, by faults in many parts of western inland Thailand, and by relatively infrequent background events in the stable interior. Figure 16 shows the contributors to 1-s seismic hazard at a site in Bangkok. Bangkok is relatively far from the nearest Quaternary fault in the fault model, the Three Pagodas fault. The main contributor to hazard in Bangkok is background seismicity in the stable Sunda plate. The 500-yr return time 1-s spectral acceleration is about 0.02 *g* in Bangkok (BC-rock site condition).

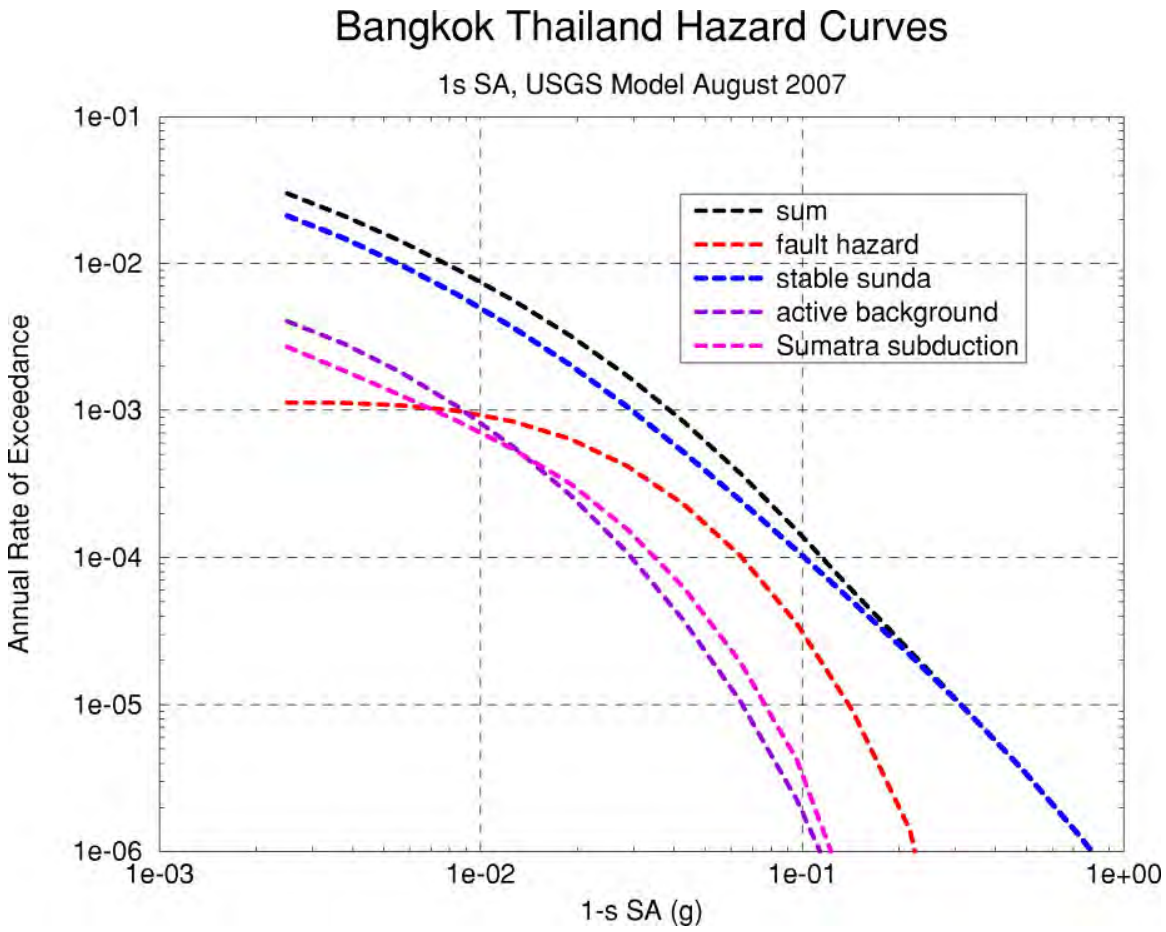

Figure 16. Hazard curves for 1-Hz spectral acceleration at a site in Bangkok, Thailand.

Conclusions

The USGS Southeast Asia seismic hazard maps are for use by USAID only. These are not ready for use in engineering design. Modification will be made to the maps to eliminate artifacts. An open-file report will be published in the near future will contains models useful for design.

References Cited

Adnan, A., and Yusof, N.A., 2001, Development of acceleration map and response spectra for seismic hazard assessment of peninsular Malaysia: Seismological Research Letters, v. 72, p. 249.

Adnan, A., Yusof, N.A., and Chink, T.N., 2002, Comparison study of several attenuation relationships for the development of seismic hazard map of Malaysia: Seismological Research Letters, v. 73, p. 238.

Allen, C.R., Gillespie, A.R., Han, Y., Sieh, K.E., Zhang, B. and Zhu, C., 1984, Red River and associated faults, Yunnan province, China—Quaternary geology, slip rates and seismic hazard: Geological Society of America Bulletin, v. 95, p. 686-700.

Ammon, C.J., Kanamori, H., Lay, T., and Velasco, A.A., 2006, The 17 July 2006 Java tsunami earthquake: Geophysical Research Letters, v. 33, L24308, doi:10.1029/2006GL028005, 5 p.

Atkinson, G.M., and Boore, D.M., 2003, Empirical ground-motion relations for subduction-zone earthquakes and their application to Cascadia and other regions: Bulletin of the Seismological Society of America, v. 93, p. 1703–1729.

Atkinson, G.M., and Boore, D. M.,2006, Earthquake ground-motion prediction equations for Eastern North America: Bulletin of the Seismological Society of America, v. 96, p. 2181–2205.

Atkinson, G.M., and Boore, D.M., 2007, Erratum—Earthquake ground-motion prediction equations for eastern North America: Bulletin of the Seismological Society of America, v. 97, p. 1032.

Beaudouin, T., Bellier, O., and Sébrier, M., 1995, Segmentation et aléa sismique sur la Grande Faille de Sumatra (Indonésie): Comptes Rendus de l'Academie des Sciences, Serie II, Sciences de la Terre et des Planetes, v. 321, no. 5, p. 409–416.

Bellier, O., Sebrier, M., Pramumijoyo, S., Beaudouin, T., Harjono, H., Bahar, I., and Forni, O., 1997, Paleoseismicity and seismic hazard along the Great Sumatran Fault (Indonesia): Journal of Geodynamics, v. 24, p. 169–183.

Bertrand, G., Rangin, C., Maury, R.C., Hla Myo Htun, Bellon, H., Guillaud, J.P., 1998, Les Basaltes de Singu (Myanmar)—Nouvelles contraintes sur le taux de decrochement recent de la faille de Sagaing [The Singu basalts (Myanmar) —New constraints for the amount of Recent offset on the Sagaing fault]: Comptes Rendus de l'Academie des Sciences, Serie II. Sciences de la Terre et des Planetes, v. 327, no. 7, p. 479–484.

Billam and others, 2005,

Bird, P., 2003, An updated digital model of plate boundaries: Geochemistry, Geophysics, Geosystems, v. 4, no. 3, 1027, doi:10.1029/2001GC000252, (*http://element.ess.ucla.edu/publications/2003_PB2002/2001GC000252.pdf*).

Boore, D., and Atkinson, G., 2007, Next generation attenuation relations to be published in Earthquake Spectra.

Bott, J., Wong, I., Prachuab, S., Wechbunthung, B., Hinthong, C., Surapiromem S., 1997, Contemporary seismicity in northern Thailand and its tectonic implications: Proceedings of the International Conference on Stratigraphy and Tectonic Evolution of Southeast Asia and the South Pacific: Bangkok, Thailand, August 19–24, 1997, p 453-464.

Building Seismic Safety Council (BSSC), 2003, 2003 Edition NEHRP recommended provisions for seismic regulations for new buildings and other structures: FEMA.

Campbell, K.W., 2002, Prediction of strong ground motion using the hybrid empirical method and its use in the development of ground-motion (attenuation) relations in eastern North America: Bulletin of the Seismological Society of America, v. 93, p. 1012–1033.

Campbell, K., and Bozorgnia, Y., 2007, Next generation attenuation relations to be published in Earthquake Spectra.

Charusiri, P., Daorerk, V., Warnichai P., Choowoing, M., Nutthee, R., Won-in, K., Surakotra, S., Singmuang, R., Jampangern, K., and Chusuthisakun, K., 2004, Executive summary report preliminary study of active fault on the Salaween Power Plant Project: Report submitted to Department of Mineral Resources, Ministry of Natural Resources and Environment, Bangkok, Thailand, 38 p.

Chiou, B., and Youngs, R., 2007, Next generation attenuation relations to be published in Earthquake Spectra.

Chlieh, M., Avouac, J.-P., Hjorleifsdottir, V., Song, T.-R. A., Ji, C., Sieh, K., Sladen, A., Hebert, H., Prawirodirdjo, L., Bock, Y., and Galetzka, J., 2006, Coseismic slip and afterslip of the great (M_w9.15) Sumatra-Andaman earthquake of 2004: Bulletin of the Seismological Society of America, v. 97, no. 1A, p. S152–S173.

Dziewonski, A.M., Chou, T.A., and Woodhouse, J.H., 1980, Determination of earthquake source parameters from waveform data for studies of global and regional seismicity: Journal of Geophysical Research, v. 86, p. 2825–2852.

Engdahl, E.R., van der Hilst, R., and Buland, R., 1998, Global teleseismic earthquake location with improved travel-times and procedures for depth determination: Bulletin of the Seismological Society of America, v. 88, p. 722–743.

Engdahl, E. R., and Villaseñor, A., 2002, Global seismicity— 1900-1999, *in* Lee, W.H.K., Kanamori, H., Jennings, P.C., and Kisslinger, C., eds., International handbook of earthquake and engineering seismology, pt. A: Amsterdam, Academic Press, p. 665–690.

Fenton, C.H., Charusiri, P., Hinthong, C., Lumjuan, A., and Mangkonkarn, B., 1999, Late Quaternary faulting in northern Thailand, in Dheeradilok, P., Hinthong, C., Chaodumrong, P., Putthapiban, P., Tansathien, W., Utha-aroon, C., Sattyarak, N., Nuchanong, T., and Techawan, S., eds., Proceedings of the International Conference on Stratigraphy and Tectonic Evolution of Southeast Asia and the South Pacific: Bangkok, Thailand, August 19–24, 1997, p 436-452.

Fenton, C.H., Charusiri, P., and Wood, S.H., 2003, Recent paleoseismic investigations in northern and western Thailand: Annals of Geophysics, v. 46, p. 957–981

Frankel, A., Mueller, C., Barnhard, T., Perkins, D., Leyendecker, E., Dickman, N., Hanson, S., and Hopper, M., 1996, National seismic-hazard maps—Documentation June 1996: U.S. Geological Survey Open-File Report 96-532, 110 p. (*http://geohazards.cr.usgs.gov/eq/html/docmaps.shtml*).

Frankel, A.D., Petersen, M.D., Mueller, C.S., Haller, K.M., Wheeler, R.L., Leyendecker, E.V., Wesson, R.L., Harmsen, S.C., Cramer, C.H., Perkins, D.M., Rukstales, K.S., 2002, Documentation for the 2002 Update of the National Seismic Hazard Maps: U.S. Geological Survey Open-File Report 02-420.

Gardner, J.K., and Knopoff L., 1974, Is the sequence of earthquakes in southern California, with aftershocks removed, Poissonian?: Bulletin of the Seismological Society of America, v. 64, p. 1363–1367.

Geomatrix Consultants, 1993, Seismic margin earthquake for the Trojan site: Final unpublished report prepared for Portland General Electric Trojan Nuclear Plant, Ranier, Oregon. (Note: tables of these attenuation relationships are included in Geomatrix consultants, 1995).

Giardini, D., 1999, The global seismic hazard assessment program (GSHAP)—1992/1999: Annali di Geofisica, v. 42, p. 957–974.

Gutenberg, B., and Richter, C.F., 1944, Frequency of earthquakes in California: Bulletin of the Seismological Society of America, v. 34, p. 185–188.

Guzman-Speziale, M., and Ni, J.F., 1996, Seismicity and active tectonics of the western Sunda arc, *in* Yin, A., and Harrison, T.M., eds., The tectonic evolution of Asia, Cambridge University Press, New York, p. 63–84.

Hinthong, C., 1995, The study of active faults in Thailand, *in* Proceedings of the Annual Technical 1995 Conference on the Progression and Vision of Mineral Resources Development.

Kastowo, D., and Gerhard, W.L., 1973, Geologic map of the Padang quadrangle, Sumatra: Geological Survey of Indonesia, Ministry of Mines Geologic Quadrangle Map, Sumatra, Padang 4/VIII, scale 1:250,000.

Kosuwan, S., Hinthong, C., Charusiri, P., 1999, The preliminary use of MapInfo programme to earthquake hazard assessment in Thailand and mainland SE Asia: Journal of Geology, Series B, no. 13–14, p. 174–178.

Kosuwan, S., Hinthong, C., Charusiri, P., 2000, The preliminary use of MapInfo programme to earthquake hazard assessment in Thailand and mainland SE Asia, *in* Proceedings of the 12th World Conference on Earthquake Engineering: New Zealand Society for Earthquake Engineering, Upper Hutt, New Zealand, v. 12, paper no. 0108.

Kosuwan, S., Saithong, P., Lumjuan. A., 2003, Paleoearthquake on the Mae Ai Segment of the Mae Chan Fault Zone, Chiang Mai, northern Thailand: Report of Geological Survey Division, Department of Mineral Resources, 57 p. (in Thai with English abstract)

Kosuwan, S., Saithong, P., Wiwegwin, W., 2006, Paleoearthquake on the Three Pagoda and Sri Sawat fault zone, Kanchana Buri, western Thailand: Report of Geological Hazard Division, Department of Mineral Resources, 100 p. (in Thai with English abstract)

LandScan™Global Population Database. Oak Ridge, TN: Oak Ridge National Laboratory. Available at *http://www.ornl.gov/landscan/*.

Lay, T., Kanamori, H., and Ruff, L., 1982, The asperity model and the nature of large subduction zone earthquakes: Earthquake Prediction Research, v. 1, p. 3–17.

Le Dain, A.Y., Tapponnier, P., and Molnar, P., 1984, Active faulting and tectonics of Burma and surrounding regions: Journal of Geophysical Research, v. 89, p. 453–472.

McCaffrey, R., 1991, Slip vectors and stretching of the Sumatran fore arc: Geology, v. 19, p. 881–884.

McCaffrey, R., and Nabelek, J., 1987, Earthquakes, gravity, and the origin of the Bali Basin—An example of a nascent continental fold-and-thrust belt: Journal of Geophysical Research, v. 92, p. 441–460.

McCue, K., 1999, Seismic hazard mapping in Australia, the Southwest Pacific and Southeast Asia: Annali di Geofisica, v. 42, no. 6, p. 1191–1197.

McGuire, R.K., 2004, Seismic hazard and risk analysis: Earthquake Engineering Research Institute MNO-10, 221 p.
Megawati, K., and Pan, T-C., Estimation of ground motion in Singapore due to a great Sumatran subduction earthquake, *in* The Eighth East Asia-Pacific Conference on Structural Engineering and Construction, Challenges in the 21st Century: EASEC-8 [electronic resource], 6 p.
Morley, C.K., 2002, A tectonic model for the Tertiary evolution of strike-slip faults and rift basins in SE Asia: Tectophysics, v. 347, p. 189–215.
Muller, J., 1895, Nota betreffende de verplaatsing van eenige triangulatie pilaren in de redidentie Tapanuli tgv. De aardbeving van 17 Mei 1892: Natuurk. Tijdschr.v. Ned. Ind., v. 54, p. 299-30.
Natawidjaja, D., Kumoro, Y., and Suprijanto, J., 1995, Gempa bumi tektonik di daerah Bukit tinggi—Muaralabuh: hubungan segmentasi sesar aktif dengan gempa bumi tahun 1926 dan 1943: Proceeding of Annual Convention of Geoteknologi-LIPI, Bandung, Indonesia.
Natawidjaja, D.H., Sieh, K., Chlieh, M., Galetzka, J., Suwargadi, B.W., Cheng, H., Edwards, R.L., Avouac, J.-P., and Ward, S.N., 2006, Source parameters of the Great Sumatran megathrust earthquakes of 1797 and 1833 inferred from coral microatolls: Journal of Geophysical Research, v. 111, B06403, doi:10.1029/2005JB004025, 37 p.
Newcomb, K.R., and McCann, W.R., 1987, Seismic history and seismotectonics of the Sunda arc: Journal of Geophysical Research, v. 92, p. 421–439.
NEHRP, 1997, NEHRP recommended provisions for seismic regulations for new buildings and other structures, 1997 edition, Federal Emergency Management Agency, FEMA 302, Feb 1998.
Pacheco, J.F., Sykes, L.R., 1992, Seismic moment catalog of large shallow earthquakes, 1900 to 1989: Bulletin of the Seismological Society of America, v. 82, p. 1306–1349.
Pailoplee., S., 2004, Thermoluminescence dating of Quaternary sediments using total bleach and regeneration methods: Chulalongkorn University, unpublished M.S. thesis.
Pan, T.C., 1997, Site-dependent building response in Singapore to long-distance Sumatra earthquakes: Earthquake Spectra, v. 13, p. 475–488.
Pan. T.C., and Sun, J., 1996, Historical earthquakes felt in Singapore: Bulletin of the Seismological Society of America, v. 86, p. 1173–1178.
Pan, T.C., Megawati, K., Brownjohn, J.M.W., and Lee, C.L., 2001, The Bengkulu, Southern Sumatra, earthquakes of 4 June 2000 (M_w = 7.7)—Another warning to remote metropolitan areas: Seismological Research Letters, v. 72, p. 171–185.
Perez, R.R., Rhodes, B.P., Liles, J.R., Lumjuan, A., Kosuwan, S, 1999, The Mae Kuang Fault; an active strike-slip fault in northern Thailand: Geological Society of America Abstracts with Programs, v. 31, no. 7, p. 428.
Petersen, M.D., Bryant, W.A., Cramer, C.H., Reichle, M.S., and Real, C.R., 1997, Seismic ground-motion hazard mapping incorporating site effects for Los Angeles, Orange, and Ventura Counties, California—A Geographical Information System application: Bulletin of the Seismological Society of America, v. 87, p. 249–255.
Petersen, M., Beeby, D., Bryant, W., Cao, C., Cramer, C., Davis, J., Reichle, M., Saucedo, G., Tan, S., Taylor, G., Toppozada, T., Treiman, J., and Wills, C., 1999, Seismic shaking hazard maps of California: California Division of Mines and Geology Map Sheet 48.

Petersen, M.D., Dewey, J., Hartzell, S., Mueller, C., Harmsen, S., Frankel, A.D., and Rukstales, K., 2004, Probabilistic seismic hazard analysis for Sumatra, Indonesia and across the southern Malaysian Peninsula: Tectonophysics, v. 390, p. 141–158.

Petersen and others, 2007, Preliminary documentation for the 2007 update of the United States National Seismic Hazard Maps, in press.

Polet, J., and Kanamori, H., 2000, Shallow subduction zone earthquake zones and their tsunamigenic potential: Geophysical Journal International, v. 142, p. 684–702.

Prawirodirdjo, L., Bock, Y., Genrich, J.F., Puntodewo, S.S.O., Rais, J., Subarya, C., and Sutisna, S., 2000, One century of tectonic deformation along the Sumatran fault from triangulation and Global Positioning System surveys: Journal of Geophysical Research, v. 105, p. 28,343–28,361.

Pubellier, M., Ego, F., Chamot-Rooke, N., and Rangin, C., 2003, The building of pericratonic mountain ranges—Structural and kinematic constraints applied to GIS-based reconstructions of SE Asia: Bulletin de la Societe Geologique de France, v. 174, p. 561–584.

Rajendran, C.P., Rajendran, K., Anu, R., Earnest, A., Machado, T., Mohan, P.M., and Freymueller, J., 2007, Crustal deformation and seismic history associated with the 2004 Indian Ocean earthquake—A perspective from the Andaman-Nicobar Islands: Bulletin of the Seismological Society of America, v. 97, p. S174–S191.

Rangin, C., Le Pichon, X., Mazzotti, S., Pubellier, M., Chamot-Rooke, N., Aurelio, M., Walpersdorf, A., and Quebral, R., 1999, Plate convergence measured by GPS across the Sundaland/Philippine Sea Plate deformed boundary—The Philippines and eastern Indonesia: Geophysical Journal International, v. 139, p. 296–316.

Replumaz, A., Lacassin, R., Tapponnier, P., Leloup, P.H., 2001, Large river offsets and Plio-Quaternary dextral slip rate on the Red River fault (Yunnan, China): Journal of Geophysical Research, v. 106, no. B1, p. 819–836.

Rhodes, B.P., Perez, R., Lamjuan, A., Kosuwan, S., 2004, Kinematics and tectonic implications of the Mae Kuang Fault, northern Thailand: Journal of Asian Earth Sciences, v. 24, p. 79–89

Rosidi, H.M.D., Tjokrosapoetro, S., and Pendowo, B., 1976, Geologic map of the Painan and northeastern part of the Muarasiberut quadrangles, Sumatra: Geological Survey of Indonesia, Ministry of Mines Geological Quadrangle Map, Sumatra, Painan-Northeastern Muarasiberut 5/VIII-4/VIII, scale 1:250,000.

Rymer, M.J., Weldon, R.J., II, Prentice, C.S., Kosuwan, S., Lumjuan, A., Muangnoicharoen, N., 1997, Tectonic setting and late Quaternary activity along the Mae Chan Fault, northern Thailand and western Laos: Geological Society of America Abstracts with Programs, v. 29, no. 6, p. 229–230.

Saithong, P., Kosuwan, S., Won-in, K., Takashima, I., Charusiri, P., 2005, Late Quaternary paleoseismic history and surface rupture characteristics of the Moei-Mae Ping fault zone in Tak Area, northwestern Thailand, *in* Proceedings of the International Conference on Geology, Geotechnology and Mineral Resources of INDOCHINA: November 28–30, 2005, Kkon Kaen, Thailand, p. 511–516.

Schoenbohm, L.M., Burchfiel, B.C., Chen, L., Yin, J., 2006, Miocene to present activity along the Red River fault, China, in the context of continental extrusion, upper crustal rotation, and lower crustal flow: Geological Society of America Bulletin, v. 118, p. 672–688.

Schwartz, D.P. and Coppersmith, K.J., 1984, Fault behavior and characteristic earthquakes—Examples from the Wasatch and San Andreas fault zones: Journal of Geophysical Research, v. 89, no. B7, p. 5681-5698.
Sieh, K., and Natawidjaja, D., 2000, Neotectonics of the Sumatran fault, Indonesia: Journal of Geophysical Research, v. 105, p. 28,295–28,326.
Sieh, K., Bock, Y., Rais, J., 1991, Neotectonic and paleoseismic studies in west and north Sumatra [abs.]: EOS [Transactions of American Geophysical Union], v. 72, no. 44, Fall meeting Supplement, p. 460.
Sieh, K., Zachariasen, J., Bock, Y., Edwards, L., Taylor, F., and Gans, P., 1994, Active tectonics of Sumatra: Geological Society of America Abstracts with Program, v. 26, no. 7, p. A-382.
Silitonga, P.H., and Kastowo, XX, 1975, Geologic map of the Solok quadrangle, Sumatra: Geological Survey of Indonesia, Ministry of Mines Geologic Quadrangle Map, Sumatra, Solok 5/VII, scale 1:250,000.
Silva, W., and others, 2005, U.S. Nuclear Regulatory Commission report.
Simons, W.J.F., Socquet, A., Vigny, C., Ambrosius, B.A.C., Abu, S. H., Promthong, Chaiwat, Subarya, C., Sarsito, D.A., Matheussen, S., Morgan, P., and Spakman, W., 2007, A decade of GPS in Southeast Asia—Resolving Sundaland motion and boundaries: Journal of Geophysical Research, v. 112, B06420, doi:10.1029/2005JB003868, 20 p.
Socquet, A., Vigny, C., Chamot-Rooke, N., Simons, W., Rangin, C., and Ambrosius, B., 2006, India and Sunda plates motion and deformation along their boundary in Myanmar determined by GPS: Journal of Geophysical Research, v. 111, B05406, doi: 10.1029/2005JB003877, 11 p.
Somerville, P., Collins, N., Abrahamson, N., Graves, R., and Saikia, C., 2001, Ground motion attenuation relations for the central and eastern United States: Final report to U.S. Geological Survey.
Tavakoli, B**.,** and Pezeshk, S., 2005, Empirical-stochastic ground-motion prediction for eastern North America: Bulletin of the Seismological Society of America, v. 95, p. 2283–2296.
Toro, G., and others, 2005, U.S. Nuclear Regulatory Commission report.
Udachachon, M., Charusiri, P., Daorerk, V., Won-in, K., Takashima, I., 2005, Paleoseismic studies along the southeastern portion of the Phrae basin, northern Thailand, *in* Proceedings of the International Conference on Geology, Geotechnology and Mineral Resources of INDOCHINA: November 28-30, 2005, Kkon Kaen, Thailand, p. 511–516.
Untung, M., Buyung, N., Kertapati, E., Undang, and Allen, C.R., 1985, Rupture along the Great Sumatran fault, Indonesia, during the earthquakes of 1926 and 1943: Bulletin of the Seismological Society of America, v. 75, p. 313–317.
Weichert, D.H., 1980, Estimation of the earthquake recurrence parameters for unequal observation periods for different magnitudes: Bulletin of the Seismological Society of America, v. 70, p. 1337–1356.
Wells, D.L., and Coppersmith, K.J., 1994, New empirical relationships among magnitude, rupture length, rupture width, and surface displacements: Bulletin of the Seismological Society of America, v. 84, p. 974–1002.

Wills, C.J., Petersen, M., Bryant, W.A., Reichle, M., Saucedo, G.J., Tan, S., Taylor, G., and Treiman, J., 2000, A site-conditions map for California based on geology and shear-wave velocity: Bulletin of the Seismological Society of America, v. 90, 6B, p. S187–S208.

Wong, I., Fenton, C., Dober, M., Zachariasen, J., and Terra, F., 2005, Seismic hazard evolution of the Tha Sae Project: Draft final report submitted to Royal Irrigation Department, Ministry of Agriculture and Cooperatives, Bangkok, Thailand.

Wood, S.H., 1995, Late Cenozoic faulting in mountainous regions of low but persistent historic seismicity—Hells Canyon (NW U.S.A.) and northern Thailand and the meaning of "active fault": IUGG XXI General Assembly, Abstracts Week B, B344.

Wood, S.H., 2001, Slip-rate estimate from offset streams, valley volumes, and denudation rate—Mae Chan Fault, northern Thailand [abs]: EOS, Transactions American Geophysical Union, v. 82, p. 932.

Youngs, R.R., Chiou, S.J., Silva, W.J., and Humphrey, J.R., 1997, Strong ground motion attenuation relationships for subduction zone earthquakes: Seismological Research Letters, v. 68, p. 58–73.

Zachariasen, J., Sieh, K., Taylor, F.W., Edwards, R.L., and Hantoro, W.S., 1999, Submergence and uplift associated with the giant 1833 Sumatran subduction earthquake—Evidence from coral microatolls: Journal of Geophysical Research, v. 104, p. 895–919.

Zhao, J., Zhang, J., Asano, A., Ohno, Y., Oouchi, T., Takahashi, T., Ogaa, H., Irikura, K., Thio, H.K., Somerville, P.G., and others, 1997, Attenuation relations of strong motion in Japan using site classification based on predominant period: Bulletin of the Seismological Society of America, v. 96, p. 898.

Appendix A. Letters of Support

ศูนย์เชี่ยวชาญเฉพาะทางด้านวิศวกรรมแผ่นดินไหวและการสั่นสะเทือน
Center of Excellence in Earthquake Engineering and Vibration

August 28, 2007

Dear Dr. Petersen,

We sincerely appreciate the great efforts and contributions of the USGS team under your leadership to develop the Probabilistic Seismic Hazard Map for Thailand. The workshop, held at Chulalongkorn University on January 16-19, 2007 was a great success. It attracted almost all Thai scientists and engineers who have been working, or who are interested to work in the future on some aspect of seismic hazard assessment or seismic design code. The technology transferred to us is really invaluable in strengthening the capacity building in seismic hazard mitigation in Thailand. The workshop, including the wrap-up one on June 29, made possible interactive input from the Thai side which, in my opinion, is beneficial for a fine tuning of the final products.

The 2004 Indian Ocean Tsunami tragedy has brought the world closer together. The collaborations of the world experts as well as the funding from USAID are gratefully acknowledged.

Yours sincerely,

Prof. P. Lukkunaprasit

To: "Prof. Panitan Lukkunaprasit" <lpanitan@chula.ac.th>

Dear Professor Panitan,

Please accept my apology for not being able to participate in the workshop on 27-30 July 2007 due to my tight schedule. From the round table discussion January, 19, the question has arisen which probability value of peak ground motion in a seismic hazard map should be adopted in the building code of Thailand. And I was appointed to have a discussion about that matter with Mr. Surachai Pornpattarakul, the director of Building Control Bureau, Department of Public Works and Town & Country Planning. The results of the discussion will be
as follow: Uniform Building Code (1985) was adopted as a model code for (1) the ministerial regulation number 49 (1997), also known as seismic code of Thailand, issued under the provision of Building Control Act, and (2) a draft of its amendment. So, our seismic zoning provisions had been established using the peak ground acceleration having a 10 % chance of being exceeded in 50 years. Building Control Bureau has a plan to revise the new seismic regulation in the near future. However, we still do not have a clear view which the direction of the revision would be. Therefore, it would be appreciated that we could have hazard maps based on both the peak ground acceleration having a 10 % and 2% chance. And we hope to adopt one of them in our building code in the future.

Thank you for your kind consideration.

Appendix B. Indonesia fault and fold database (west of long. 115° E)

No.	Structure Name	Segment	Location			Quality of location[a]	Structure_Att			Length (km)	Large Historical Earthquakes / Year(M)	Geomorphic Features	M_{Max}[1]	M_{Max}[2]	Slip Rate by Geol. data (mm/yr)	Slip rate source	Slip Rate by GPS (mm/yr)	Geodetic rate source	Recurrence Interval (yr)
			Y1	Y2	Province		Type	Strike	Dip_angle										
1	Sumatran Fault	Sunda	-6.75	-5.9	--	Fair	Dextral	170	~90	150	No record	submarine graben	7.6	7.7	n/a		n/a		
2		Semangko	-5.9	-5.25	Lampung	Good	Dextral	142	~90	65	1908	east facing scarp	7.2	7.2	n/a		n/a		
3		Kumering	-5.3	-4.35	Bengkulu; Sumatera Selatan; Lampung	Good	Dextral	134	~90	150	1933(Ms=7.5)/1994(Mw=7.0)	Suoh geo thermal valley	7.6	7.7	n/a		n/a		
4		Manna	-4.35	-3.8	Bengkulu	Good	Dextral	134	~90	85	1893	mountain ous range on east side of the fault, associated with possible folds and thrusts	7.3	7.4	n/a		n/a		
5		Musi	-3.65	-3.25	Bengkulu	Good	Dextral	144	~90	70	1979(Ms=6.6)	valley, depression	7.2	7.3	11	Sieh et al, 1994; Sieh and Natawidjaja, 2000	n/a		
6		Ketaun	-3.35	-2.75	Bengkulu	Good	Dextral	138	~90	85	1943(Ms=7.3)/1952(Ms=6.8)	depression valley and Kaba volcano	7.3	7.4	11	Sieh et al, 1991; Sieh et al, 1994	n/a		
7		Dikit	-2.5	-2.4	Jambi	Good	Dextral	140	~90	60	no record	n/a	7.2	7.2	11	Sieh et al, 1991; Sieh et al, 1994	n/a		
8		Siulak	-2.25	-1.7	Sumatera Barat	Good	Dextral	142	~90	70	1909(Ms=7.6)/1995(Mw=7.0)	Lake Kerinci and Kunyit volcano	7.2	7.3	11	Sieh et al, 1991; Sieh et al, 1994	23	Prawirodirdjo et al, 2000	
9		Suliti	-1.75	-1	Sumatera Barat	Good	Dextral	144	~90	95	1943(Ms=7.4)	small depression, calderas and young volcanic cone	7.4	7.4	11	Sieh et al, 1991; Sieh et al, 1994	23 ± 5	Genrich et al, 2000	
10		Sumani	-1	-0.5	Sumatera Barat	Good	Dextral	148	~90	60	1943(Ms=7.6)/1926(Ms~7)	Lake Diatas, calderas and Talang volcano	7.2	7.2	11	Sieh et al, 1991; Sieh et al, 1994	23	Prawirodirdjo et al, 2000	
11		Sianok	-0.7	0.1	Sumatera Barat	Good	Dextral	146	~90	90	1822/1926 (Ms~7)	Lake Singkarak	7.3	7.4	11	Sieh et al, 1991; Sieh et al, 1994	23 ± 3	Genrich et al, 2000	
12		Sumpur	0	0.3	Sumatera Barat	Good	Dextral	155	~90	35	no record	wide depression associated with normal faults	6.9	6.9	n/a		n/a		
13		Barumun	0.3	1.2	Sumatera Utara	Good	Dextral	137 to 162	~90	125	no record	long (Sumpur) valley along the fault	7.5	7.6	n/a		n/a		

14		Angkola	0.3	1.8	Sumatera Utara	Good	Dextral	155 to 127	~90	160	1892(Ms=7.7)	mountainous ranges on both sides of the fault	7.6	7.7	n/a		23 ± 4	Genrich et al, 2000	
15		Toru	1.2	2	Sumatera Utara	Good	Dextral	145	~90	95	1984(Ms=6.4)/1987(Ms=6.6)	uplifted hill on the east side of the bend	7.4	7.4	n/a		24	Prawirodirdjo et al, 2000	
16		Renun	2	3.5	Sumatera Utara	Good	Dextral	140	~90	220	1916/1921 (mb=6.8)/1936(Ms=7.2)	Tarutung Valley	7.8	7.9	27	Sieh et al, 1991	24 ± 1 - 26 ± 2	Genrich et al, 2000	
17		Tripa	3.4	4.4	Aceh	Good	Dextral	127	~90	180	1990(Ms=6?)/1997(Mw=6?)	Alas Valley	7.7	7.8	n/a		n/a		
18		Aceh	4.4	5.4	Aceh	Good	Dextral	130	~90	200	no record	mountainous range, associated with active thrusts	7.7	7.9	38 ± 4	Bennett et al, 1981	n/a		
19		Seulimeum	5	5.9	Aceh	Good	Dextral	145	~90	120	1964(Ms=6.5)	Small depression on dilatational stepover	7.5	7.6	38 ± 4	Bennett et al, 1981	13	Genrich et al, 2000	
20	Toru fold and thrust belt		1	1.5	Sumatera Utara	Good	Fold	150	--	50	no record	Swamp and Folded Mio-Pliocene sediment	7.1	7.1	n/a		n/a		

.

Appendix C. Hazard Maps for Sumatra and Java, Indonesia

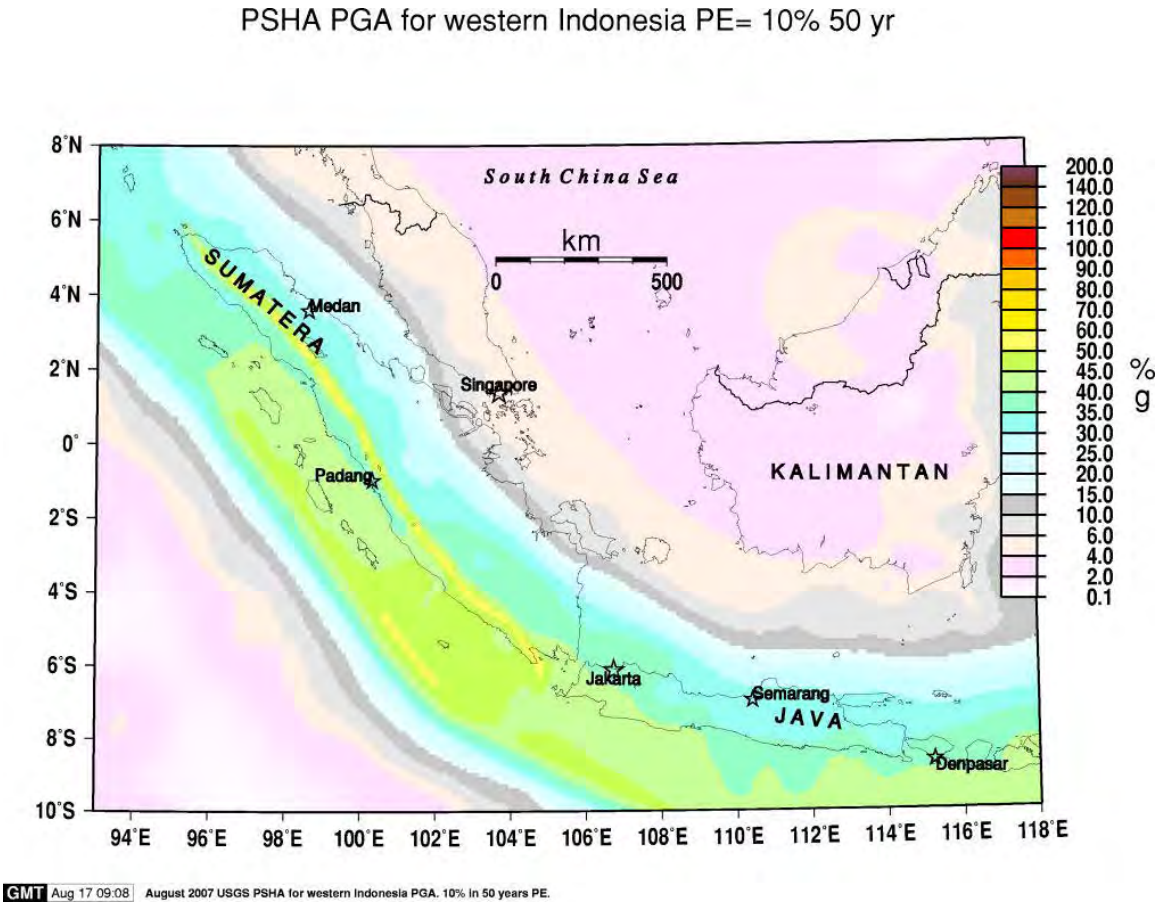

Figure C-1. Hazard map for Sumatra and Java, Indonesia showing the peak ground acceleration with a 10-percent probability of exceedance in 50-yr hazard level for firm rock site condition (Vs30=760 m/s). Low areas near Borneo are artifacts of the Sunda zone and will be modified in the near future.

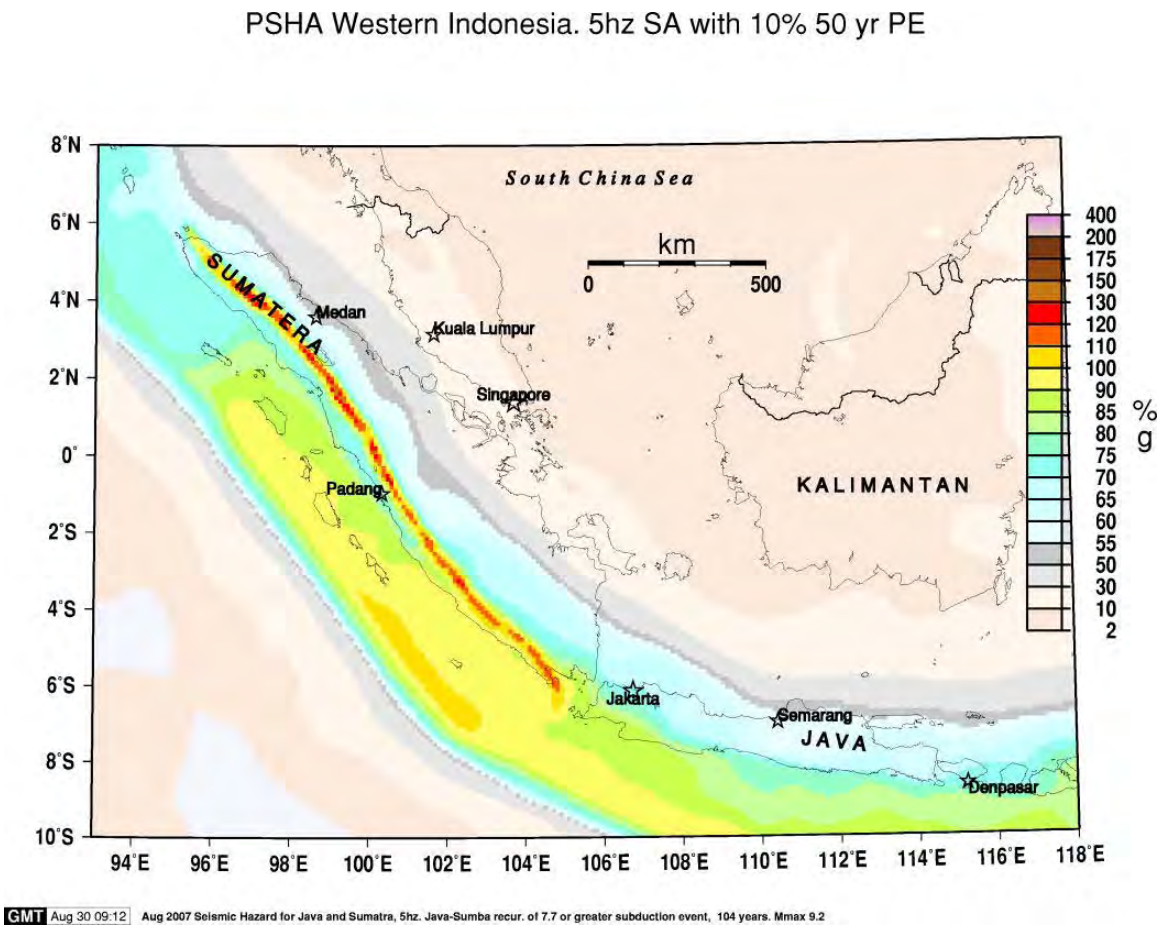

Figure C-2. Hazard map for Sumatra and Java, Indonesia showing the 5-Hz spectral acceleration with a 10-percent probability of exceedance in 50-yr hazard level for firm rock site condition (Vs30=760 m/s). Low areas near Borneo are artifacts of the Sunda zone and will be modified in the near future.

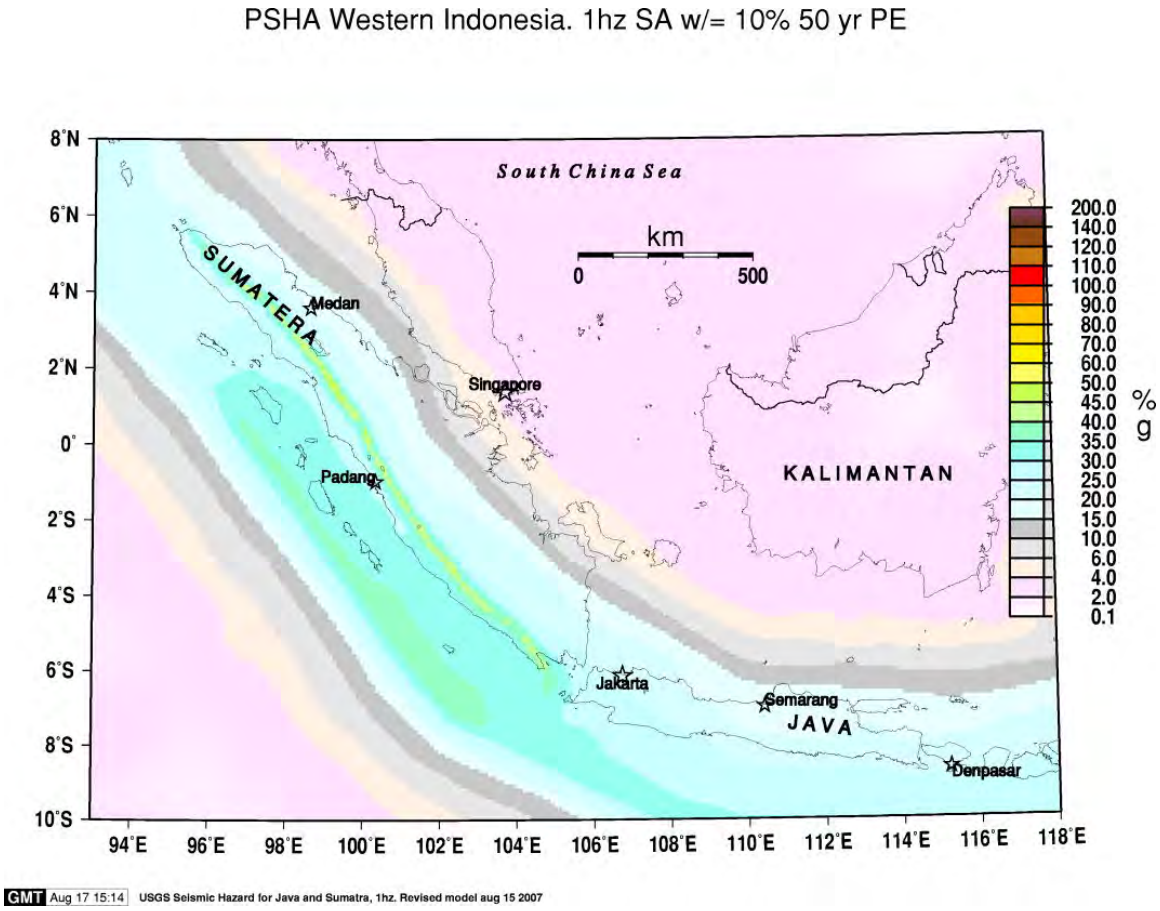

Figure C-3. Hazard map for Sumatra and Java, Indonesia showing the 1-Hz spectral acceleration with a 10-percent probability of exceedance in 50-yr hazard level for firm rock site condition (Vs30=760 m/s). Low areas near Borneo are artifacts of the Sunda zone and will be modified in the near future.

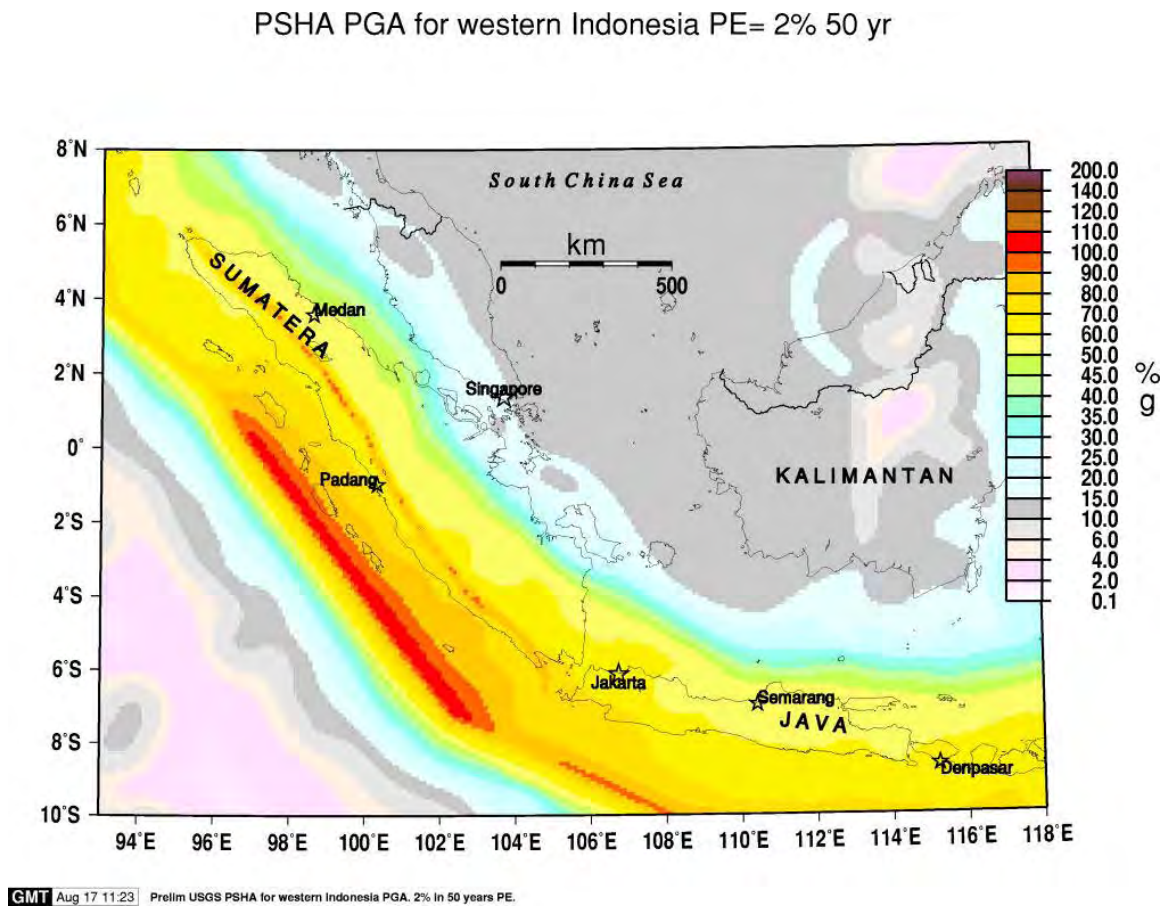

Figure C-4. Hazard map for Sumatra and Java, Indonesia showing the peak ground acceleration with a 2-percent probability of exceedance in 50-yr hazard level for firm rock site condition (Vs30=760 m/s). Low areas near Borneo are artifacts of the Sunda zone and will be modified in the near future.

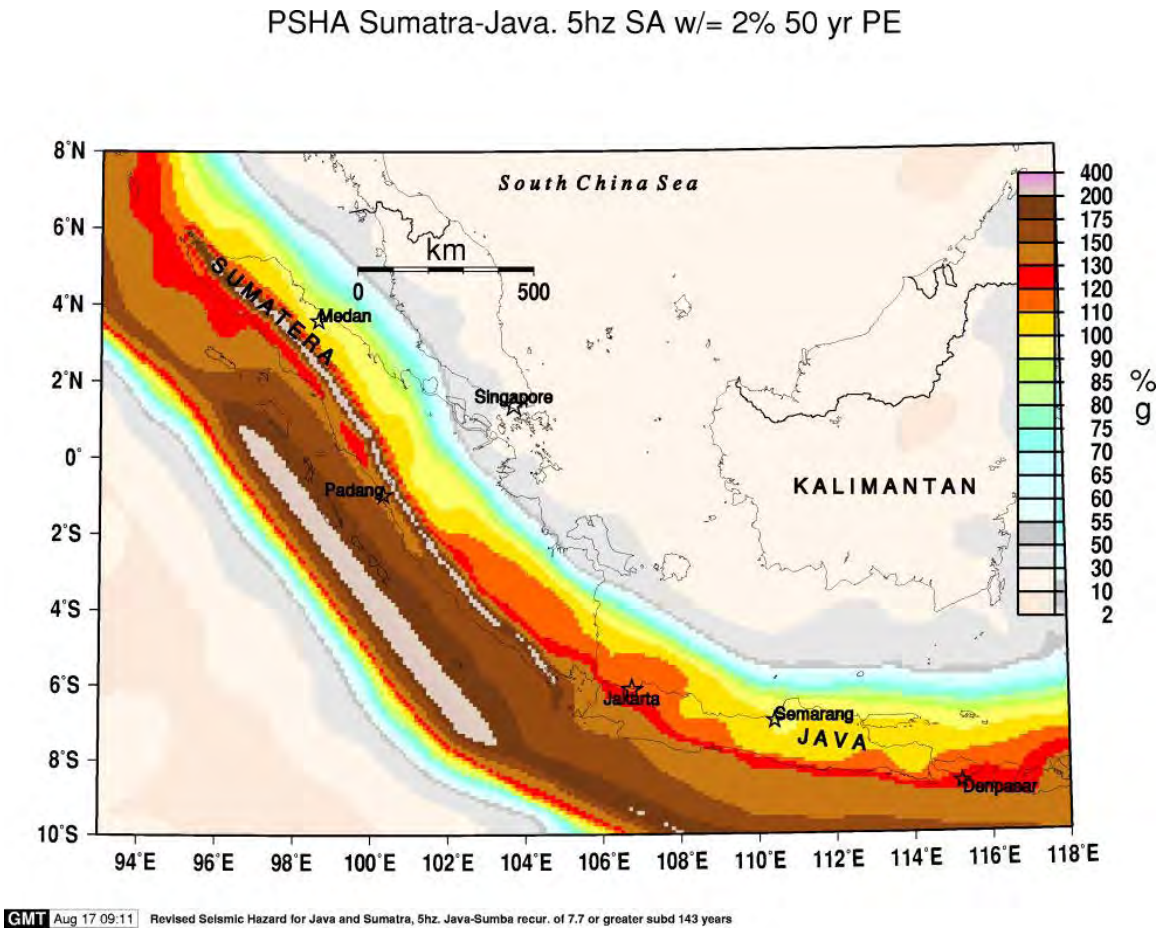

Figure C-6. Hazard map for Sumatra and Java, Indonesia showing the 5-Hz spectral acceleration with a 2-percent probability of exceedance in 50-yr hazard level for firm rock site condition (Vs30=760 m/s). Low areas near Borneo are artifacts of the Sunda zone and will be modified in the near future.

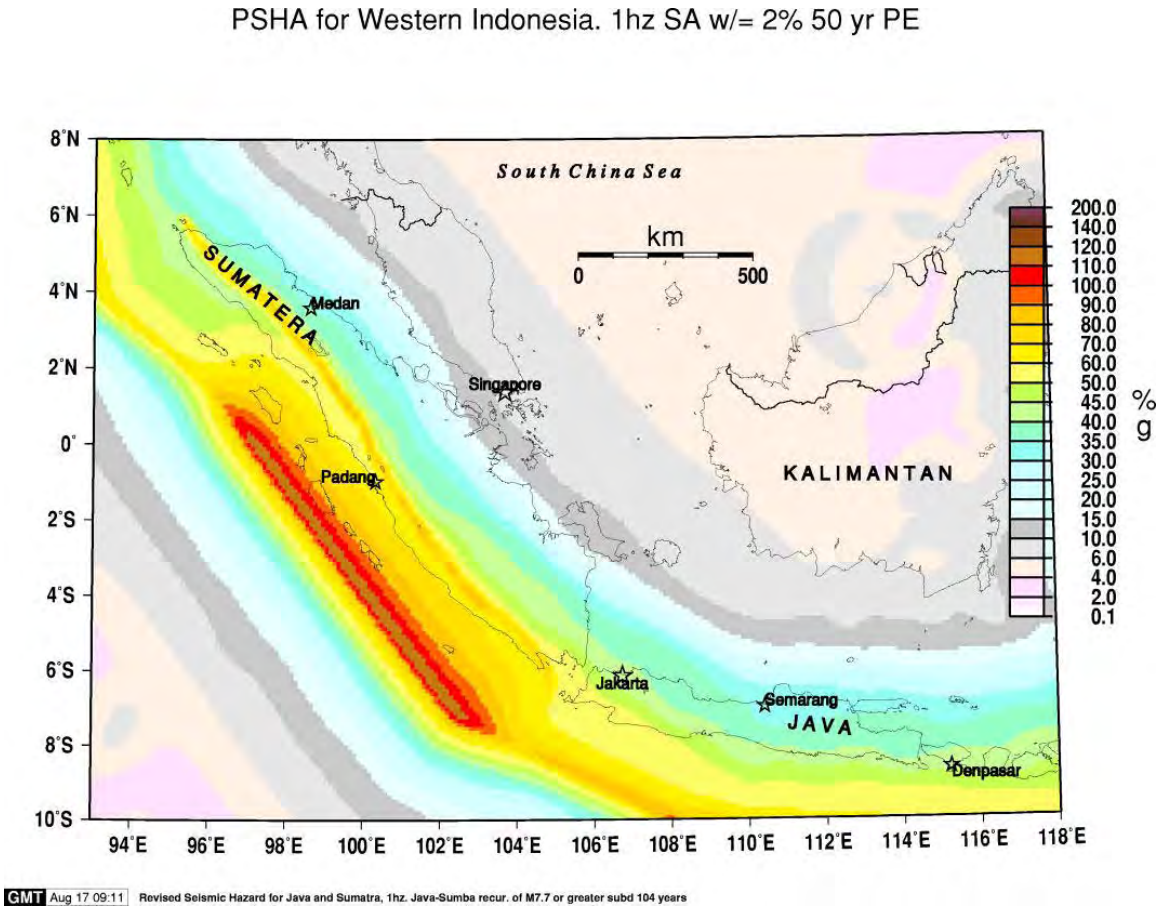

Figure C-5. Hazard map for Sumatra and Java, Indonesia showing the 1-Hz spectral acceleration with a 2-percent probability of exceedance in 50-yr hazard level for firm rock site condition (Vs30=760 m/s). Low areas near Borneo are artifacts of the Sunda zone and will be modified in the near future

Appendix D. Hazard Maps for Thailand and Malaysian Peninsula

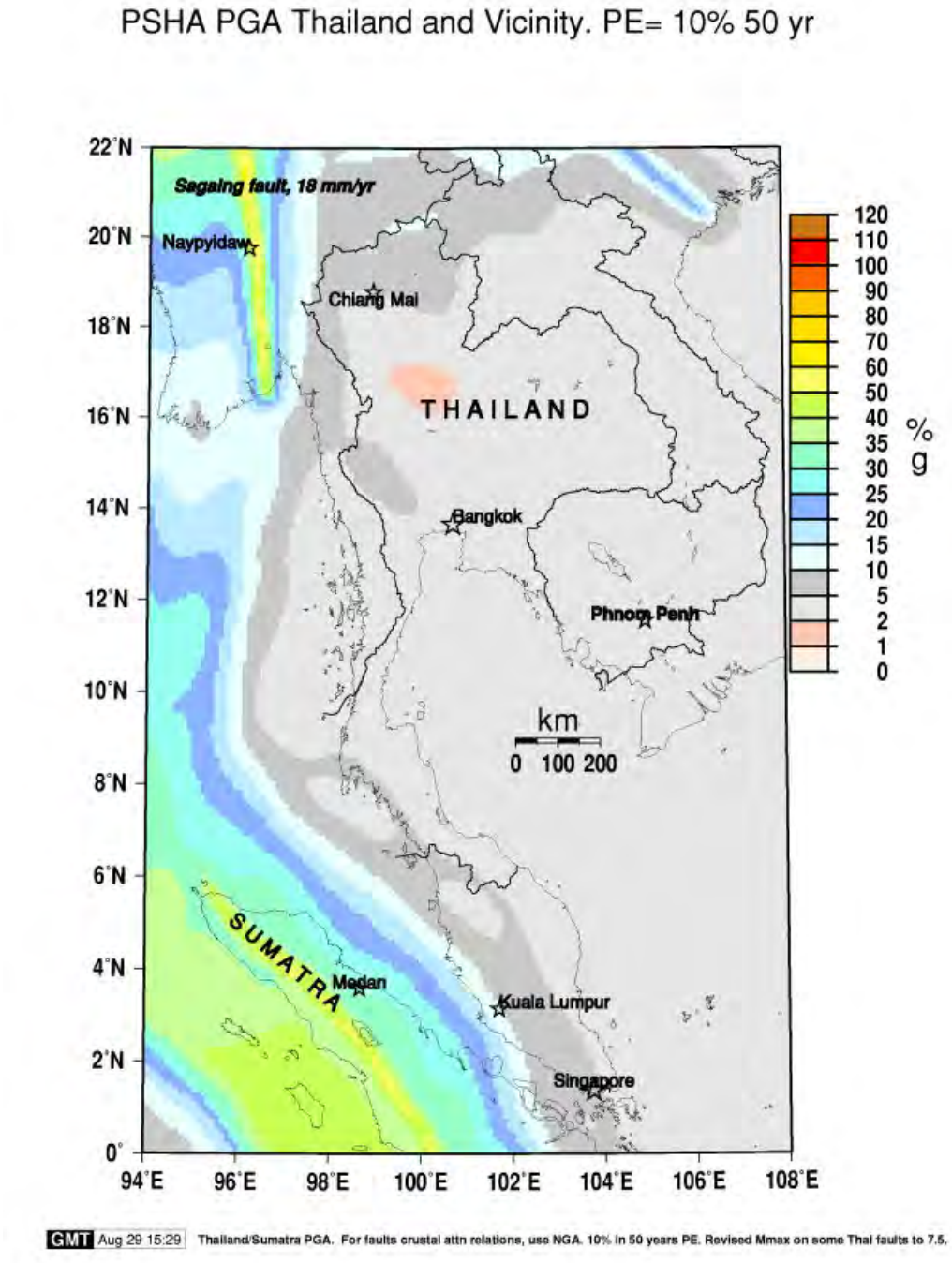

Figure D-1. Hazard map for Thailand and Malaysian peninsula showing the peak ground acceleration with a 10-percent probability of exceedance in 50-yr hazard level for firm rock site condition (Vs30=760 m/s). Low hazard areas near central Thailand are artifacts of the Sunda zone and will be modified in the near future.

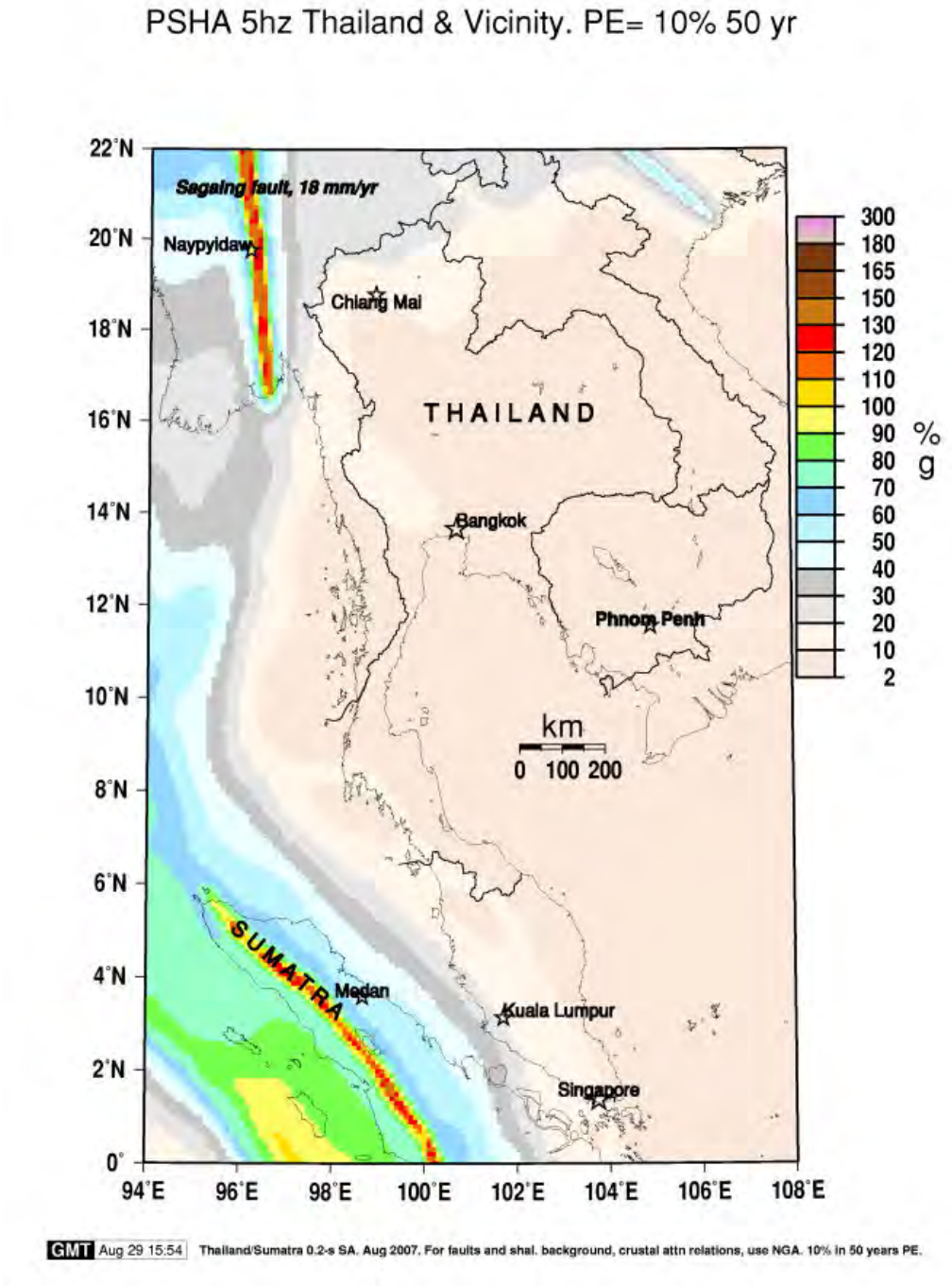

Figure D-2. Hazard map for Thailand and Malaysian peninsula showing the 5-Hz spectral acceleration with a 10-percent probability of exceedance in 50-yr hazard level for firm rock site condition (Vs30=760 m/s). Low hazard areas near central Thailand are artifacts of the Sunda zone and will be modified in the near future.

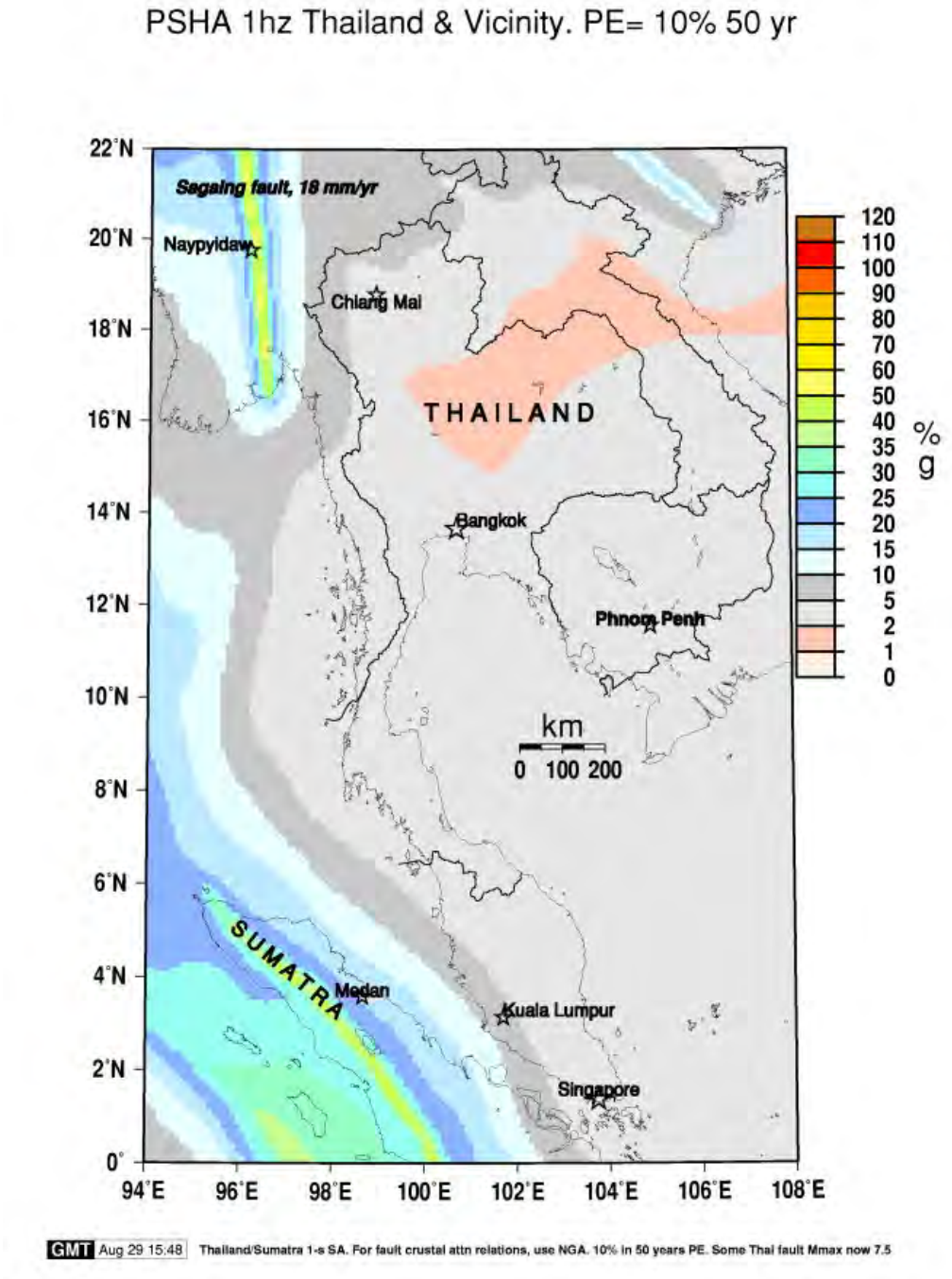

Figure D-3. Hazard map for Thailand and Malaysian peninsula showing the 1-Hz spectral acceleration with a 10-percent probability of exceedance in 50-yr hazard level for firm rock site condition (Vs30=760 m/s). Low hazard areas near central Thailand are artifacts of the Sunda zone and will be modified in the near future.

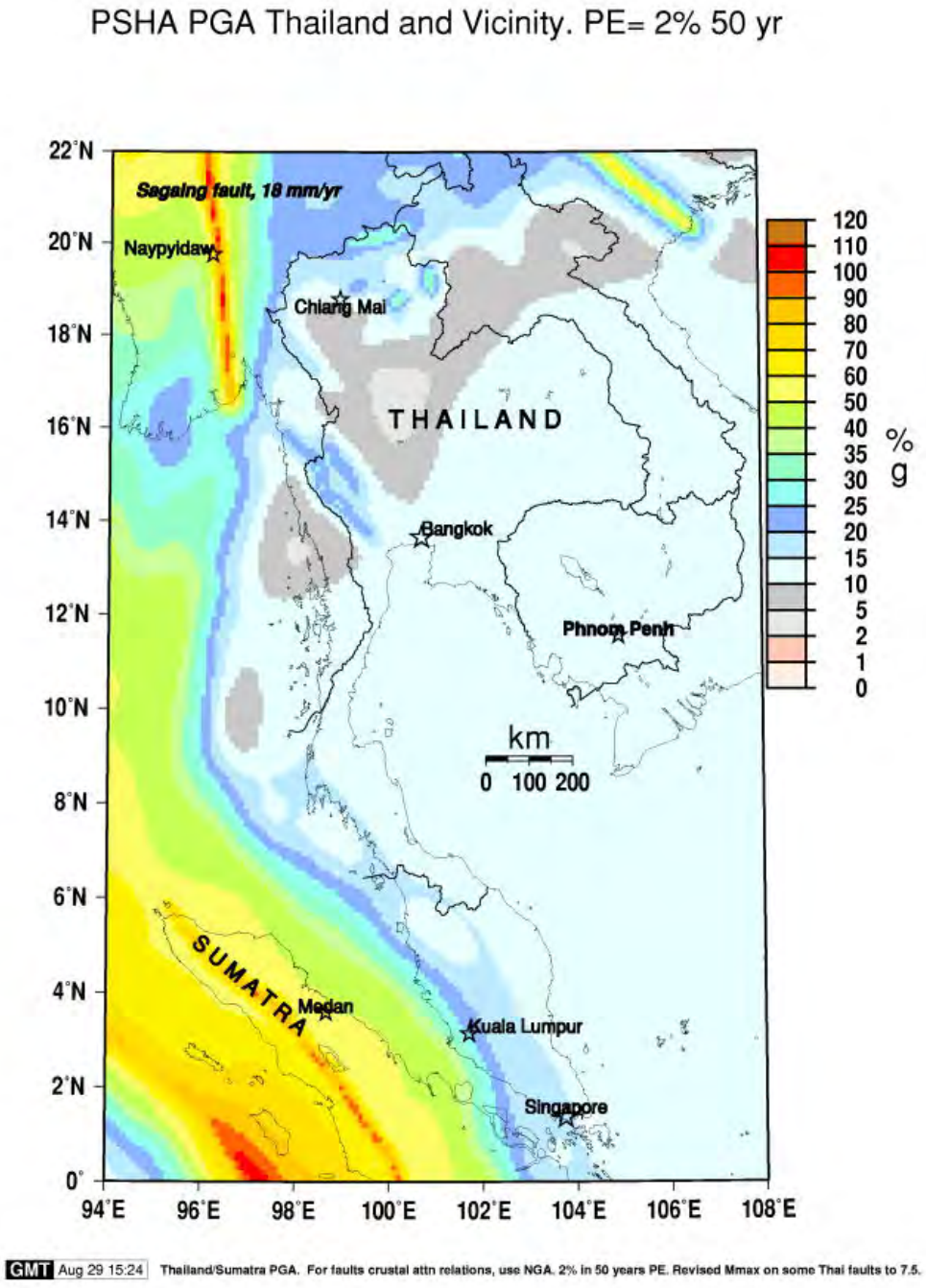

Figure D-4. Hazard map for Thailand and Malaysian peninsula showing the peak ground acceleration with a 2-percent probability of exceedance in 50-yr hazard level for firm rock site condition (Vs30=760 m/s). Low hazard areas near central Thailand are artifacts of the Sunda zone and will be modified in the near future.

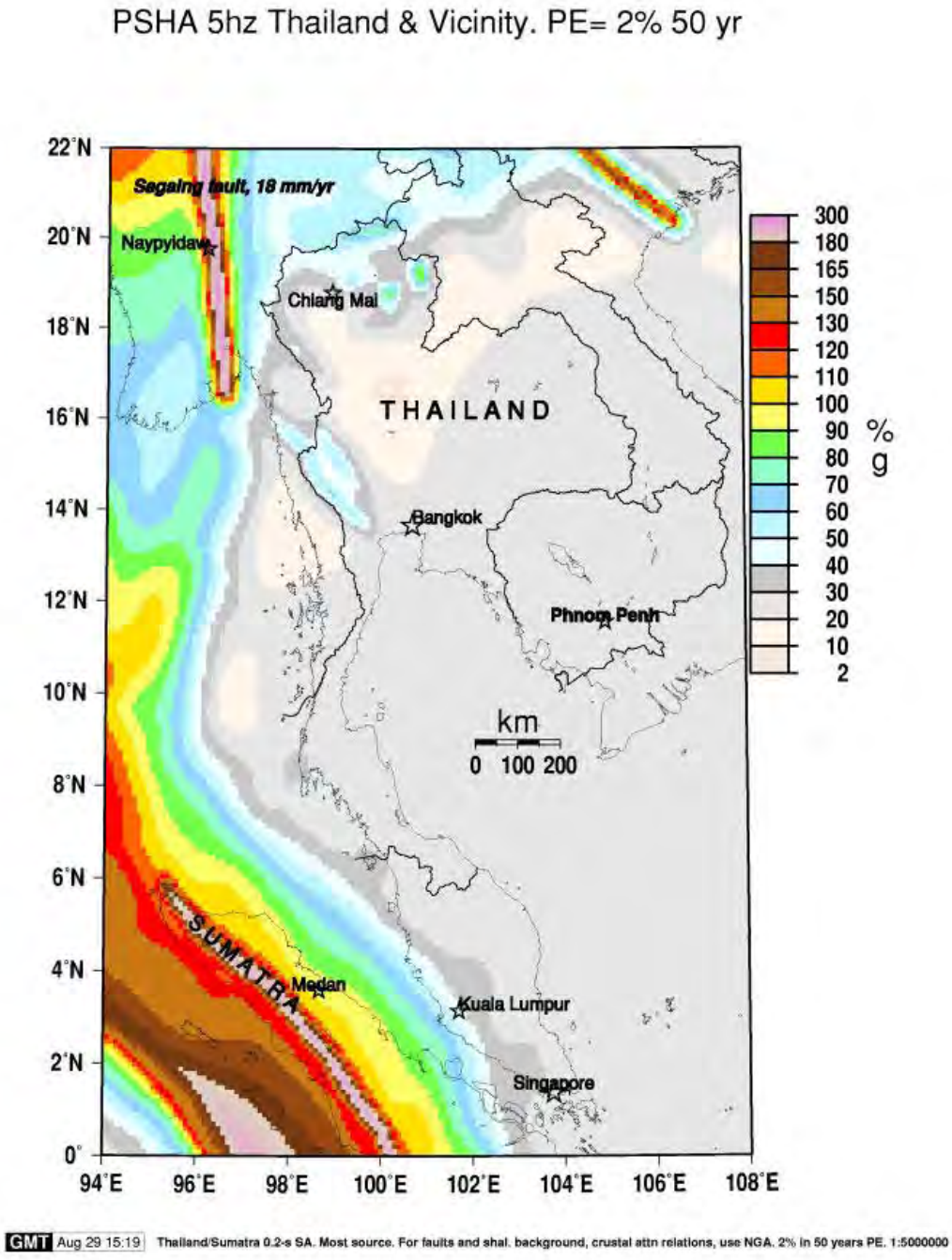

Figure D-5. Hazard map for Thailand and Malaysian peninsula showing the 5-Hz spectral acceleration with a 2-percent probability of exceedance in 50-yr hazard level for firm rock site condition (Vs30=760 m/s). Low hazard areas near central Thailand are artifacts of the Sunda zone and will be modified in the near future.

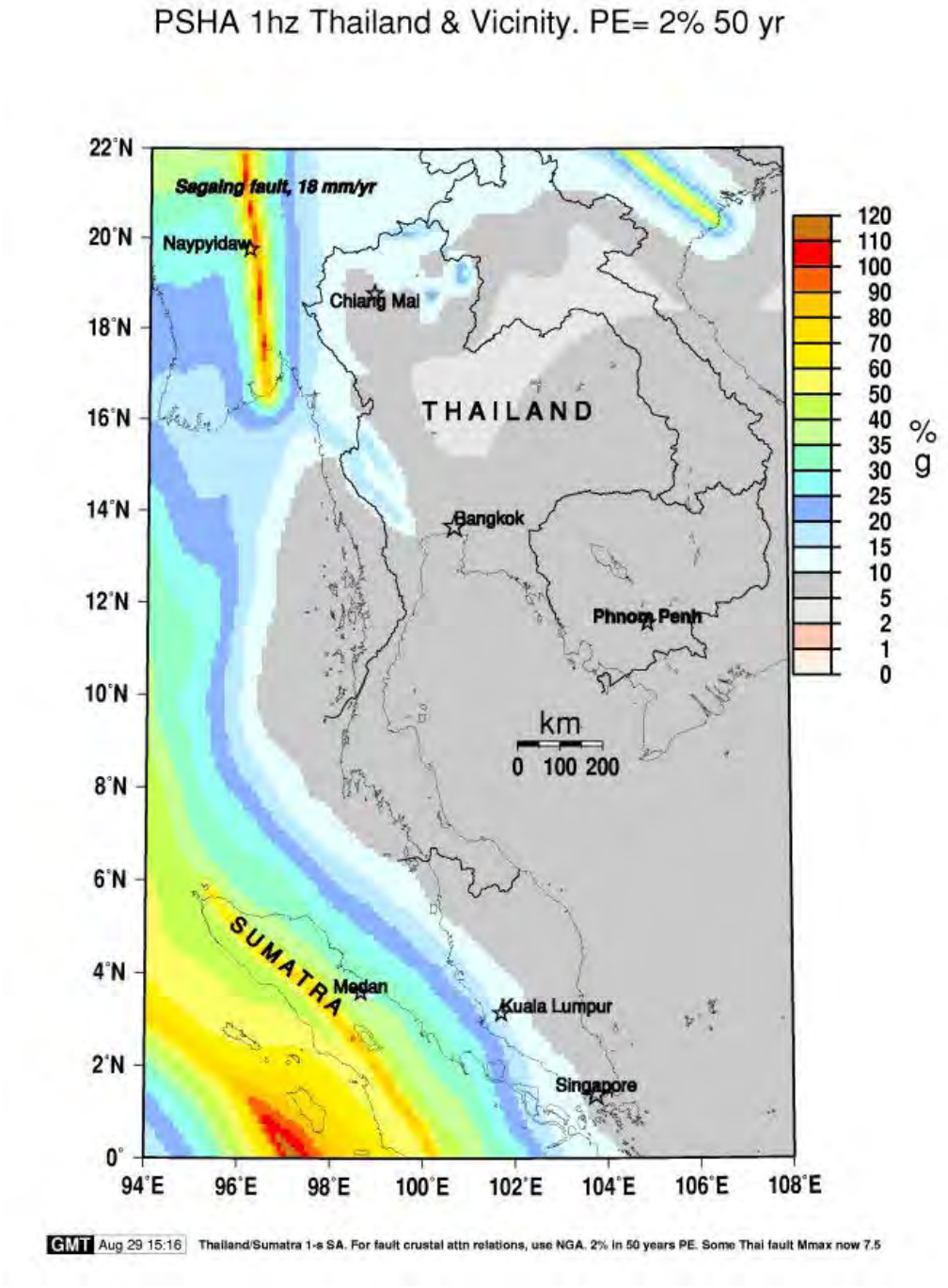

Figure D-6. Hazard map for Thailand and Malaysian peninsula showing the 1-Hz spectral acceleration with a 2-percent probability of exceedance in 50-yr hazard level for firm rock site condition (Vs30=760 m/s). Low hazard areas near central Thailand are artifacts of the Sunda zone and will be modified in the near future.